Martinez Sanchez, A.H.; Luthringer, B.J.C.; Feyerabend, F.; Willumeit, R.:

Mg and Mg alloys: How comparable are in vitro and in vivo corrosion rates? A review

In: Acta Biomaterialia (2014) Elsevier

DOI: 10.1016/j.actbio.2014.11.048

Mg and Mg alloys: How comparable are *in vitro* and *in vivo* corrosion rates? – A Review

Adela Helvia Martinez Sanchez, Bérengère J.C. Luthringer, Frank Feyerabend, Regine Willumeit

Institute of Materials Research, Department for Structural Research on Macromolecules, Helmholtz-Zentrum Geesthacht (HZG), Geesthacht, Germany

* Please address correspondence to:
Adela Helvia Martinez Sanchez; E-mail: adela.martinez@hzg.de;
Telephone: 0049 4152 87 2591; Fax: 0049 4152 87 2666

*Graphical Abstract

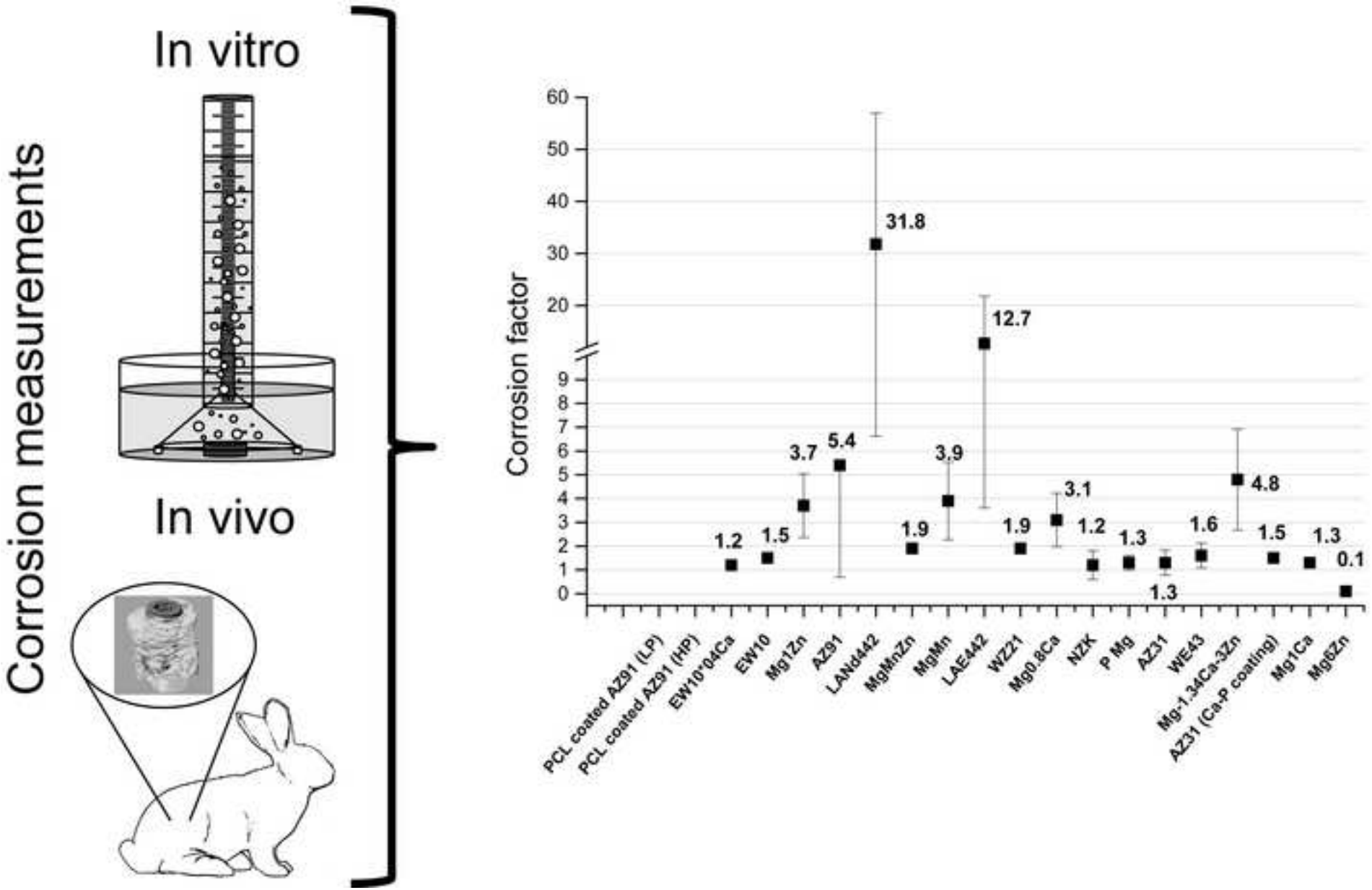

Abstract

Due to their biodegradability, magnesium and magnesium based alloys could represent the third generation of biomaterials. However, their mechanical properties and time of degradation have to match application needs. Several approaches, such as choice of alloying elements or tailored microstructure, are employed to tailor corrosion behaviour. Due to the high electrochemical activity of Mg, numerous environmental factors (e.g., temperature and surrounding ion composition) are influencing its corrosion behaviour causing its unpredictability. Nevertheless, the need of reliable in vitro model(s) to predict in vivo implant degradation is increasing. In attempt to find a correlation between in vitro and vivo corrosion rates, this review presents a systematic literature survey as well as an attempt to correlate the different results.

117 words

Keywords: magnesium alloys; in vitro and in vivo corrosion; biomaterials; orthopaedics; biodegradable metallic implants

1 Introduction

Mg and its alloys have been extensively investigated in recent decades due to several properties that make them promising candidates for biodegradable materials for medical applications. These materials exhibit biocompatibility and appropriate mechanical properties for use, for example, as orthopaedic implants [1]. Furthermore, Mg and Mg alloys can corrode completely under physiological conditions, avoiding the need for a second surgical intervention to remove the implant after bone healing.

The great challenge here is to tailor the degradation in a manner that is suitable for a biological environment. Fast or uncontrolled corrosion is associated with strong hydrogen and ion release and severe pH changes, which can lead to undesirable biological reactions [2]. In parallel, a loss of mechanical stability before complete bone healing is observed. Therefore, the correct way of producing a Mg implant for orthopaedic applications remains under discussion [3].

One of the approaches employed to control corrosion behaviour is tailoring the composition and microstructure, including the grain size and texture of the base material. Such tailoring can be achieved by alloying or developing optimised manufacturing methods and post-processing techniques such as heat-treatment [4-6] and other strategies such as the development of porous structures or composites [7-10]. Another approach is the use of surface coatings, which can also increase the biocompatibility of medical devices [11, 12].

In addition to these attempts to improve corrosion resistance, the fundamental problem remains: metallic corrosion is an electrochemical process that involves reduction and oxidation reactions. Similar to other metals, the corrosion resistance of magnesium (Mg) or Mg alloys is influenced by the surrounding environment; therefore, it is important to note that *in vivo*, the corrosion will be determined mainly by the place of implantation (and the corresponding body fluids flow and composition), whereas *in vitro*, the environmental conditions are defined mainly by the corrosion solution employed.

Furthermore, as corrosion is an electrochemical reaction, further influencing factors such as temperature alter its degradation kinetics.
Due to the high electrochemical activity of Mg, the relative importance of some environmental factors is greatly amplified (*e.g*., the ion content in the surrounding fluids) [13].
Therefore, one of the most exigent problems concerning Mg and Mg alloys is the unpredictable corrosion behaviour *in vivo*, where numerous ions are present in body fluids (*e.g.,* Na, K, Ca, Mg, HCO_3, Cl, HPO_4 and SO_4) and make metallic corrosion very hard to predict or define [14]. Additionally, thus far, no correlation between *in vitro* and *in vivo* corrosion rates has been presented, which proves the need for (I) improved *in vitro* models that mimic as close as possible the *in vivo* conditions, (II) the identification of factors influencing corrosion rate *in vitro* that can help to predict *in vivo* degradation behaviour and (III) the identification of corrosion mechanisms *in vivo*. The latter is especially difficult to determine because the monitoring of degradation as well as physiological parameters *in vivo* and online is more or less impossible at the current stage.
A substantial number of scientific publications regarding the degradation of Mg and its alloys have reported a large range of results due to the different materials, methods and experimental conditions selected. To the best of our knowledge there has not been a systematic approach or agreement on the experimental conditions to study Mg degradation that could bridge the gap between laboratory results and performance in a living organism. Instead, it has been concluded that it is impossible to compare these conditions to find consistent limits for prediction of the corrosion rate of Mg alloys *in vivo*, which are considered the only reliable data [15]. Still, to make the laboratory experiments meaningful and to avoid unnecessary animal experiments, at least some type of correlation should be defined or a recommendation should be given under which experimental conditions are best comparable.
This review is a systematic literature survey that provides an overview of the existing results for *in vitro* and *in vivo* corrosion rates and aims to evaluate the existence or lack of correlation between the *in vitro* and *in vivo* corrosion behaviour of Mg and Mg alloys. In an attempt to quantify such a possible correlation, the corrosion factor, which describes the ration between the corrosion rate *in vitro* and the corresponding value obtained *in vivo*, was calculated.
An exhaustive survey of parameters influencing the corrosion rate is not the focus of this review. For instance, the effect of alloying elements, heat treatments, processing and coatings (used *in vivo* and *in vitro)* will not be considered. Nevertheless, the effect of some selected parameters on the corrosion rate that is determined by the environment will be discussed: (1) the selection of the corrosion solution and (2) the implantation site.

2 Bibliographic selection of *in vivo* data

A complex bibliographic survey was necessary to select the information for comparison of the corrosion behaviour of the different Mg alloys.
The starting point was collection of all the publications regarding the corrosion rate of Mg and Mg alloys for orthopaedic applications *in vivo*.

Of the 50 animal studies (since the first use in 1900 by Pyer [16] until today [17]), 30 were not considered due to lack of quantitative information about the corrosion rate (or insufficient data to calculate the rate). This result already highlights one severe problem: the great variety of possible parameters that are monitored during *in vivo* trials but not necessarily the corrosion rate.
The remaining publications contained information for approximately 23 different Mg alloys and pure Mg (PMg) (Table 1). These alloys were implanted mainly in the femur or tibia of three animal models: rabbit, rat and guinea pig. In some cases, the implants were located intramedullary, while in other cases, the implant was only in contact with cortical bone. Implants were even located subcutaneously in some studies. We are well aware that the implantation site – whether surrounded by blood, soft or hard tissue– significantly affects the corrosion rate. Nonetheless, when comparing the corrosion rates for one specific material, the rates are not very different or at least the differences cannot be attributed to the implant location (Table 1).

Among all the aspects affecting the results obtained *in vivo*, Table 1 highlights two remarkable ones that appear to cause large variability: method and time period considered to measure the corrosion rate.

2.1 Methods used to calculate the corrosion rate *in vivo*

There are several available approaches to estimate the corrosion rate *in vivo*: *via* weight loss – which is strictly speaking not an *in vivo* method - or *via* volume loss. To calculate the weight loss, the implant must be removed from the implantation site (see Table 2). Recent studies commonly employed micro computed tomography (µCT) [18-20], allowing the calculation of the implant volume changes. The reduction in implant volume obtained from 3D µCT images can be converted into a general corrosion rate using a modification of the weight loss method. For better resolution, µCT is also performed *ex vivo* after removing the implant and bone from the animal. However, with better instrumentation, it is now also possible to follow the degradation process *in vivo* [20] and to differentiate the corrosion layer and the degraded implant from the surrounding tissues.
Some studies provided semi-quantitative or qualitative data [21-23] to evaluate *in vivo* corrosion (*i.e.,* giving a score value from 0-4 depending on the degree of degradation), which were not included in this review.

2.2 Periods considered to measure the corrosion rate *in vivo*

The periods used to measure the corrosion rate *in vivo* vary from a few days to more than one year. Consequently, the determined *in vivo* corrosion rates exhibit a broad variability depending on the time at which the corrosion rate was detected. For example, the corrosion rates of ZX50 without and with a surface treatment were calculated from volume loss by µCT after 1, 2, 3, 4, 8 and 12 weeks [24]. Without surface treatment, during the first 4 weeks after implantation, the corrosion rate remained unchanged at 1.7 mm/year but exhibited almost a two-fold increase to 3 mm/year after 8 weeks and to 4 mm/year after 12 weeks. For the treated ZX50 alloy, the initial corrosion rate was much lower (0.25 mm/year) and increased gradually until a final corrosion rate of 6 mm/year was reached after 12 weeks. If we only considered the corrosion rate obtained

after 3 weeks, both materials would have the same corrosion rate, but as deduced from the previous data, this analysis is not a true representation of the corrosion behaviour of these alloys (treated ZX50 was completely degraded after 12 weeks, while untreated ZX50 remained almost intact).
Due to the variability depending on the time considered and to the fact that there are not common points for all the Mg alloys (some studies are longer than others), an overall corrosion rate *in vivo* was calculated for every material as the average of all the corrosion rates at different time points. The corresponding error bar considered the severe variations over time points. This estimation is only a very rough approach to reach comparability with *in vitro* results. However, these systematic problems were also observed for *in vitro* measurements which supports the need for unified test procedures.

3 Bibliographic selection of *in vitro* data

In a subsequent step, *in vitro* studies with the same alloys as identified from the *in vivo* experiments were selected (Table 3). As expected, the number of available publications was much higher, also implying a higher variability in experimental set-ups. For two novel alloys (ZEK100 and AX30) that were tested *in vivo*, information regarding the corrosion rate *in vitro* is not yet available in the literature [25]. Therefore, this work summarises the corrosion rates both *in vitro* and *in vivo* for 20 materials.
We are aware that the technique used to determine the corrosion rate, the corrosion medium and various other parameters (*e.g.*, temperature) affect the degradation of the material.

3.1 Methods used to calculate corrosion rates *in vitro*

Depending on the method employed to evaluate the corrosion rate *in vitro* (*i.e.*, electrochemical tests, hydrogen evolution or mass/volume loss after immersion test), a large range of results for the same alloy can be achieved. The methods and corresponding equations used for *in vitro* testing are summarised in Table 2. Evaluation of the mass/volume loss, pH monitoring or hydrogen evolution all require a low cost and are methods that are easily performed. Electrochemical tests are simple to perform, highly reproducible, and suitable for qualitative studies of corrosion and more commonly, for mechanistic studies of the corrosion behavior [26, 27]. Potentiodynamic polarization (PDP) is the most frequently used electrochemical technique for studying in vitro corrosion of Mg alloys [26, 28-69]. Electrochemical impedance spectroscopy (EIS), is another technique that has been widely used for evaluating corrosion of biomaterials [30, 31, 33, 35, 38, 44-46, 48-54, 56-58, 60-62, 64, 66, 69-82].

However, it is important to note that electrochemical tests must be performed during short testing times, leading to accelerating corrosion situations that do not simulate the true corrosion situation *in vivo* [27, 83] and limit the correlation with the corrosion rate obtained from the other methods after longer periods of time [26].
Furthermore, the mass or volume loss methods are more similar to the ones employed *in vivo* (previously discussed). As an example of the different results obtained using different *in vitro* methodologies, Table 4 lists the corrosion rate of Mg and three different alloys obtained in two studies [84, 85]. Thus, only the corrosion rates obtained *via* mass or volume loss, and hydrogen evolution were further considered for evaluating the

correlation *in vitro-in vivo*. Nevertheless, corrosion rates obtained with electrochemical tests (previously converted to corrosion rates in mm/years by the authors), are also included in table 3. A deeper analysis about the limitations and benefits of this (and other) methods can be found in Kirkland *et al.,* 2012 [83].

Table 4 also demonstrates the effect of calculating the corrosion rate by mass-loss measurements without removing the corrosion products [86] that can lead to a negative rate. The comparability of *in vitro* corrosion was difficult because the rates were provided in different units, as parts per million (ppm) of Mg ion released to the corrosion solution [85, 87], mg/cm^2 day [18, 73, 88, 89], and percentage of weight or volume loss [21, 84, 90-92] among others.
In this study, the corrosion rates were then all converted to mm/year, as this unit is the most frequently used unit observed in the literature. However, when the corrosion rates were expressed as percentage of weight or volume loss, or even as remaining volume after test, the initial dimensions of the sample were necessary and sometimes missing. Therefore, these measurements were also discarded**.**

3.2 Periods considered to measure the corrosion rates *in vitro*

As mentioned above, the time at which the corrosion rate is determined is crucial and this is also true for *in vitro* measurements. Most of the studies considered corrosion rates as a constant; however, a more detailed time-dependent study can show that the corrosion rate is not linear over time due to, for example, the formation of a protective corrosion layer on the material surface [93, 94]. Furthermore, alloying elements can increase the complexity of the time-dependent corrosion behaviour. Time points from 10 hours [87] to 18 weeks [90] are presented in this review.
Some materials exhibit a high initial corrosion rate that decreases with immersion time due to the gradual formation of a protective layer that can only be detected when considering several time point measurements. Such a non-monotonic behavior has been confirmed by AC impedance measurements and explained by the competition between formation of a Ca-containing film and degradation of the original film [95].
To illustrate the high variability of corrosion rates depending on the immersion time as an example, in two studies, the corrosion rate of AZ31 (high purity; commercial) was observed over 20 days (data shown in Table 3). The authors determined the corrosion rate after 1, 2, 5, 10, 15 and 20 days [96] or after 5 and 20 days [93]. In both publications, the corrosion rate decreased from day 5 to day 20 by approximately 0.3 mm/year. However, in the more detailed study, it was possible to determine a linear decrease, while linearity could not be confirmed in the second study. Notably, Yibin et al. calculated the corrosion rate of AZ31 up to 30 days (after 2, 5, 10, 20 and 30 days), which revealed an increase of the corrosion rate after 20 days and modified the overall estimation of the corrosion behaviour. Furthermore, the author stipulated that the corrosion rate of the alloy was 0.3 mm/year, which corresponds to the corrosion rate after 10 days of immersion test, while the average calculated (from the different time points) would be 0.75 mm/year. Although the differences in material processing in both studies should also be considered, it is easy to appreciate how different the information obtained from the corrosion rate can be, depending on the time-points considered.

As previously explained for *in vivo* corrosion rates, common time points for all the materials are missing among all the studies. To overcome this problem and to allow for data comparison, in this paper, the overall corrosion rate was calculated as the average of the corrosion rate obtained at different time points.

4 Correlation in vitro - in vivo:

After the complex selection process of data, the average corrosion rates of 19 Mg alloys and pure Mg are finally included in this paper (Table 5). An overview of the results is presented in Fig. 1 as the average corrosion rate ± standard error. Each point in the graph represents the average corrosion rate for one of the material, calculated from the corrosion rates at different time points and collected from different studies. In addition, different implantation sites and corrosion media were included in that average. We are aware that by combining all these various parameters, we are making systematic assumption. However, it appears surprising that the overall calculated corrosion rates exhibit relatively small variations from one material to another, mostly being less than 2 mm/year (apart from results from electrochemical tests, where as previously mentioned, an accelerated corrosion rate is induced) and rather homogeneous, which justifies our approach to some extent.
As depicted in Fig. 1, it can be observed that the corrosion rate *in vivo* is described by a smaller range of values than is the *in vitro* corrosion rate. *In vivo*, the corrosion rates range from 0 to 1.5 mm/year (except Mg6Zn: 2.3 mm/year), whereas *in vitro*, the corrosion rates, even if exhibiting more exceptions, range mainly from 0.1 to 2 mm/year. LANd442 exhibited the highest *in vitro* corrosion rate (8.8 mm/year); however, its corrosion was studied only in Seitz *et al.* [86] (*in vitro* in SBF). The corrosion rate of LAE442 (3.9 ± 1.5 mm/year) and Mg-1.34Ca-3Zn (4.5 mm/year) are also exceptions; however, it is important to note the high standard error associated with the LAE442 corrosion rate.
For all the Mg and Mg alloys represented in this review (except Mg6Zn), the *in vivo* corrosion rates are lower than are the *in vitro* ones.

In an attempt to quantify the correlation between the *in vitro* - *in vivo* corrosion rates, the corrosion factor (cf) *was* calculated by dividing the overall corrosion rate *in vitro* by the overall corrosion rate *in vivo* (Eq. 1). In the calculation of the corrosion factor, error propagation was included. Because the *in vitro* corrosion rates were usually higher, the resulting corrosion factor was >1 in most of the cases.

$$cf = (X \pm dX) / (Y \pm dY) = (X / Y) \pm dZ \qquad \text{(Eq. 1)}$$

Where:

X: Average corrosion rate *in vitro*
dX: Standard error of corrosion rate *in vitro*
Y: Average corrosion rate *in vivo*

dY: Standard error of corrosion rate *in vivo*
dZ: Error propagation

Fig. 2 demonstrates that most of the corrosion factors are contained in a small range, varying mainly from 1 to 4.9. These values indicate that the possible corrosion rate *in vivo* on average 1 - 5 times lower than the corrosion rate obtained *in vitro*. As expected, some exceptions are observed: for Mg6Zn, the corrosion factor is lower than 1 (0.06). Other exceptions are both HP- and LP-coated AZ91, which are nearly stable *in vivo* (corrosion rate of approximately 0). Therefore, the corresponding corrosion factors are not shown in Fig. 2, as they are not relevant (105 and infinite, respectively, which is not representative of the real corrosion behaviour). LAE442 and LANd442, as expected from their high *in vitro* corrosion rate, also exhibited high corrosion factors (12.7 ± 9.1 and 31.8, respectively).
The relatively close correlation between the *in vitro* and *in vivo* corrosion rate was not obvious from the initial literature survey, and it is immanent that a clustering of values even below 2.5 can be observed. Upon closer examination, this finding could be correlated to the solution that was used in the *in vitro* measurements.

5 Correlation of the corrosion factor with the *in vitro* corrosion solution

To find systematic correlations, we studied the corrosion factors with respect to the material, temperature during measurements, implantation site and corrosion medium. As expected, no correlation was observed for the material (results not shown). Here, the statistics were too poor because, in general, only one data set per material was available, and no systematic assessment of changes in the material properties due to different treatments was performed. For the same reason, a systematic comparison of the correlation between the microstructure and the deviations of the *in vitro* and *in vivo* corrosion rates was impossible.
When evaluating the effect of the animal model or implantation side on the corrosion rate, no systematic deviation of the corrosion factor was detected (results not shown).
It should be noted that not all the materials included in this review were tested with all the mediums; thus, only those materials that allowed the most complete data sets were considered. We did not consider measurements performed in NaCl solutions, which are the most widely used *in vitro* corrosion conditions. Here, the drawback is that so many different NaCl concentrations were used that the statistics were insufficient because of only one data point per condition.
However, when the corrosion factors were grouped according to the corrosion media, EBSS, SBF, Hank´s solution, MEM, and MEM with the addition of BSA employed for *in vitro* tests, a correlation became visible (Fig. 3). We observed that – apart from a few exceptions – the corrosion factors obtained for a specific corrosion solution were rather similar. For EBSS and SBF, the corrosion factors are below 3, while for MEM, the factors are higher and more in the range between 1.5 – 3.5. The addition of proteins increased these values to a range between 4 and 7. Hank's solution resulted in very different corrosion factors; due to a lack of statistics, it is difficult to judge if a correlation can be observed.

These results indicate that upon using the correct corrosion solution (and considering most likely a few other factors such as temperature, CO_2 content or maybe flow), it should be possible to approach corrosion values *in vitro* that reliably predict the behaviour *in vivo*.

6 Discussion

This study demonstrates that the overall corrosion rate *in vitro* was in general higher than the corrosion rate obtained *in vivo* and that the corrosion factors are similar when considering some of the media used for *in vitro* assessment of the degradation. For most materials, the results obtained *in vitro* and *in vivo* are grouped in a much narrower range than initially expected.

Why are corrosion rates measured *in vitro* and *in vivo* different even for the same material, and is there any opportunity to obtain a better correlation? We must address methodological and systematic deviation and a severe lack of knowledge.

As noted, the measurement of corrosion rates can be performed using several methods, and the results are not necessarily comparable. We can observe the systematic problem that it can be difficult to distinguish *in vivo* between the metal, the corrosion layer and the surrounded tissue. Some software used to calculate the corrosion rate *in vivo* cannot precisely define these limits, generating a non-reliable corrosion rate [97]. Then, the temperatures used to determine the corrosion rate are usually not in the physiological range. The effect of temperature on the corrosion rate has been demonstrated in several publications *in vitro* [98]. Kirkland *et al*. [83] observed that with high-purity Mg, the corrosion rate measured at 37°C (simulated body temperature) was twice higher than that measured at 20°C (room temperature). Furthermore, these authors also demonstrated that with a temperature increase of only 3°C (from 37°C to 40°C), the corrosion rate was increased by approximately 50%, foretelling a potential risk of a too fast initial corrosion rate of the materials after implantation.

One of the major obstacles for comparability is the use of synthetic corrosion solutions *in vitro* that simulate the *in vivo* environment [56, 85, 94, 99-101]. The compositions of some of the solutions used for *in vitro* tests are listed in Table 6. The general opinion is that the corrosion solution should be as close as possible to physiological conditions. Therefore, a simple solution of chlorides does not represent the chemical environment that the material will find in the body. Thus, the use of more realistic media such as simulated body fluids (SBF), MEM, Dulbecco´s modified eagle medium (DMEM), Hank's solution, and artificial plasma (AP) to measure mass loss are widely used (*e.g*., Kirkland *et al*. [102]). Our analysis revealed that especially Earle´s balanced salt solution (EBSS), MEM and SBF result in a relatively good correlation between *in vitro* and *in vivo* results. SBF has precisely the same carbonate content as blood plasma and a very similar amount of other inorganic ions. EBSS and MEM contain a slightly lower amount of carbonate ion and more notable differences for other ions such as Ca and Mg.

In addition to the composition of the corrosion medium, the presence of a buffering system has a large effect on the corrosion rate, as it is important to keep the pH constant around the materials [32, 56, 103, 104]. Non-buffered solutions allow a pH increase towards the basic regime, which leads to passivation due to the formation of protective layers. Among the buffer systems available for testing *in vitro* corrosion of

biomaterials, $NaHCO_3/CO_2$ buffers are the most similar to the system found *in vivo*. It has been shown that the choice of a more "bio"realistic buffer will give rise to a behavior of the corrosion layers (and therefore the corrosion behaviour) closer to the one observed *in vivo* [105].
Layers such as crystalline $Mg(OH)_2$, amorphous phosphate-containing and amorphous carbonated (Mg-Ca)-phosphate layers (with poor protective properties) form in the presence of NaCl and $NaCl^+$ Ca, $NaCl^+PO_3$, SBF, respectively [106]. If the pH is maintained in the neutral regime – as occurs *in vivo* – the corrosion will not be stopped.
Apart from the corrosion solution, new approaches are being investigated, leading in some cases to corrosion behaviours further from the behaviour observed *in vivo*: among others, the use of dynamic test conditions should mimic the *in vivo* environment even better. Nevertheless the results obtained with AZ31 under both static and dynamic conditions [44] indicate a higher corrosion rate under dynamic conditions (1.5 mm/year with dynamic tests and 0.3 mm/year in static tests), differing more from the results obtained *in vivo* (corrosion rate of less than 1 mm/year). Furthermore, the corrosion kinetics over time appear to be affected by the dynamic conditions: in static medium *in vitro*, the corrosion rate tends to decrease at the beginning (high corrosion resistance) and then to increase with time. This result may be due to the formation of a protective layer [95]. In dynamic fluid tests, the corrosion rate does not tend to decrease with time because the protective layer cannot be formed [93]. In addition, with the aim of better simulating *in vivo* conditions, Schinhammer et al. used gaseous CO2 in SBF to keep the pH constant, avoiding the need of a buffer. Nonetheless, the *in vitro* degradation rate of the alloy WZ21 (0.8 mm/year) was more than twice the corrosion rate obtained *in vivo* (0. 36 mm/year) [107].

Why is a lower corrosion rate observed *in vivo* for most of the materials? One possible explanation is the lower concentration of chloride ions present in blood plasma (103 mM) [108] and bone (48.6-56.7 mM) [99] than in SBF (147.8 mM) and in other commonly used media [31].

Organic components, such as proteins and amino acids, lead to different corrosion behaviours. Proteins and amino acids in biological fluids are hypothesised to form an absorbed layer on the surface of Mg alloys that can lead to different responses depending on the alloy composition [29, 53, 75]. Other studies propose that proteins are not adhering but interfere in a chemical manner by changing the density and composition of the corrosion layer as a whole [109]. In PMg and LAE442, the presence of proteins accelerates the corrosion rate, while in other cases, such as in AZ31, AZ91 and MgCa, their presence resulted in no effects or even a decrease in the corrosion rate. Another study demonstrated that the addition of bovine serum albumin (BSA) to MEM medium increases the corrosion rate of most of the tested alloys; however, for Mg1.34Ca3Zn, the effect was again a decrease [104]. This contradictory effect can be explained as follows. First, the corrosion rate decrease may be due to the protective layer formed between the metal and the surroundings [110], which can inhibit the effect of a pH change and hinder the diffusion of ions [56]. In addition, the corrosion rate increase may be explained by the fact that proteins may complex metal cations and

accelerate the dissolution of Mg alloys. It has even been suggested that proteins can remove the oxide layer [111, 112] formed on the surface of the materials.
In summary, organic and inorganic components as well as buffers systems have a clear effect on the corrosion rate of Mg-based materials; however, the results obtained *in vitro* and *in vivo* are controversial mainly due to the interaction of several conditions that are highly variable from one case to another.

In addition, the physiological environment and the capacity of the body to adapt to changing environmental conditions is a severe reason for the differences.

One of the environmental factors affecting the corrosion rate *in vivo* is the anatomical location of the implant. Differences in the flow rates, water content of tissues or hydrogen diffusion coefficients in different animal models have already been noted [113]. However, our analysis revealed that when comparing averaged corrosion rates, the order of changes in the corrosion rate is negligible.

The instability of the *in vivo* corrosion layer has been suggested as another factor explaining the differences between *in vivo/in vitro* corrosion rates. $Mg(OH)_2$ is one of the main components observed in the corrosion layer and is not stable in aqueous solutions, especially not in chloride-containing environments [85, 114]. As a chemical reaction, the corrosion of the Mg alloy would cease when an equilibrated concentration of ions is reached in the surrounding fluid. However, under *in vivo* conditions, the electrolyte concentrations are subjected to homoeostasis, and equilibrium is never reached, leading to the complete material corrosion [115].
Additionally, local changes in electrochemical conditions could also be caused by locally passivated areas that are covered by newly formed bone, which have been observed by µCT. These locally different corrosive environments could cause local anodic and cathodic sites, which could in turn lead to an accelerated corrosion rate following the morphology of pitting corrosion [85]. Thus, another proposed reason for the lower corrosion rate obtained *in vivo* could rely on the response of the host tissue to the surgical procedure and the presence of the material itself (*e.g*., inflammation and foreign body reaction): an initial pH decrease directly after surgery can result in a short-term enhancement of the corrosion rate, with the consequent formation of a stable corrosion layer, which reduces the corrosion rate of the implants (as time goes on). Nevertheless, these physiological reactions will dynamically change over time and depend on the type of surrounding tissue, affecting not only the pH but other important parameters such as the ion concentration and temperature and subsequently the corrosion rate [116]. Another proposed reason (which remains tentative) is the suppression of micro-galvanic corrosion *in vivo*, possibly due to the encapsulation of the material by the surrounding tissues [117].

In general, we must state that there is a lack of information about human physiology that leads to unexpected corrosion behaviours. It has been previously reported that even when the implantation location is the same and the alloy has the same composition, the results regarding corrosion rate and hydrogen production can differ. Witte *et al.* [94] reported that the intramedullary implantation of AZ91 Mg alloy into guinea pig femora

resulted in gas formation, with bubbles appearing within one week of implantation and disappearing after two to three weeks. In contrast, Wong *et al*. [18] could not detect gas formation during the entire period of study. This example demonstrates how important it is to decide how *in vivo* studies should be performed, perhaps even down to the surgical technique employed.

7 Summary

The differences between corrosion behaviour *in vitro* and *in vivo* (even with the same material composition) can be attributed mainly to the difficulties in mimicking the complex physiological conditions *in vitro*.

Lack of information and the highly variable methodological procedures in previous studies are some of the factors that limit the comparison of the corrosion behaviour. Some of the *in vivo* studies focus only on qualitative aspects, while a quantitative study is missing. Furthermore, some of the studies *in vitro* and *in vivo* do not provide the corrosion rate or sufficient information to calculate this rate (for example, the alloy density or sample dimensions are missing).

The use of some standardised methods or common protocols for measuring the corrosion rate as well as common time points and a more detailed explanation about all the parameters used during experimental corrosion rate evaluation are key factors to allow comparison between results obtained and to improve our understanding about the complex corrosion behaviour of Mg and Mg alloys both *in vitro* and *in vivo*. Perhaps a round robin laboratory approach would be very helpful for this aim.

Nevertheless, from the data collected in this review, two main facts can be noted: the first one is that in addition to the high variability in experimental set-ups when considering the overall corrosion rates for all the materials (both *in vitro* and *in vivo),* the variability is not as large as could be expected. The corrosion rates *in vivo* are lower for all the alloys and PMg (apart from one exception), showing a *in vitro-in vivo* correlation*.* Furthermore, when calculating the *in vitro-in vivo* corrosion factor*,* a systematic ratio was detected that varies mainly from approximately 1 to 5 units, indicating a possible corrosion rate *in vivo* between 1 and 4 times lower than the corrosion rate *in vitro*.

This range of values is even reduced when selecting the right medium for *in vitro* testing (a reduction towards 1-3 units), indicating the existence of a systematic correlation. This correlation is more obvious when using media that better mimic physiological conditions (such as SBF, EBSS or MEM).

Acknowledgements

This work was supported by Helmholtz Virtuelles Institut, VH-VI-523 In vivo studies of biodegradable magnesium based implant materials „MetBioMat". The µCT image in the graphical abstract was kindly supplied by SCANCO Medical AG, Brüttisellen, Switzerland (http://www.scanco.ch/en/docs/images/microct40.html)

References

[1] Waizy H, Seitz J-M, Reifenrath J, Weizbauer A, Bach F-W, Meyer-Lindenberg A, et al. Biodegradable magnesium implants for orthopedic applications. J Mater Sci 2013;48:39-50.

[2] Virtanen S. Biodegradable Mg and Mg alloys: Corrosion and biocompatibility. Materials Science and Engineering: B 2011;176:1600-8.
[3] Garg S, Bourantas C, Serruys PW. New concepts in the design of drug-eluting coronary stents. Nature reviews Cardiology 2013;10:248-60.
[4] Liu C, Xin Y, Tang G, Chu PK. Influence of heat treatment on degradation behavior of bio-degradable die-cast AZ63 magnesium alloy in simulated body fluid. Materials Science and Engineering: A 2007;456:350-7.
[5] Wang Y, Liu G, Fan Z. A new heat treatment procedure for rheo-diecast AZ91D magnesium alloy. Scripta Materialia 2006;54:903-8.
[6] Zeng R-c, Zhang J, Huang W-j, Dietzel W, Kainer KU, Blawert C, et al. Review of studies on corrosion of magnesium alloys. Transactions of Nonferrous Metals Society of China 2006;16, Supplement 2:s763-s71.
[7] Li N, Zheng Y. Novel Magnesium Alloys Developed for Biomedical Application: A Review. Journal of Materials Science & Technology 2013;29:489-502.
[8] Wen CE, Mabuchi M, Yamada Y, Shimojima K, Chino Y, Asahina T. Processing of biocompatible porous Ti and Mg. Scripta Materialia 2001;45:1147-53.
[9] Wen CE, Yamada Y, Shimojima K, Chino Y, Hosokawa H, Mabuchi M. Porous Bioresorbable Magnesium as Bone substitute. Materials Science Forum 2003;419:1001-6.
[10] Wen CE, Yamada Y, Shimojima K, Chino Y, Hosokawa H, Mabuchi M. Compressibility of porous magnesium foam: dependency on porosity and pore size. Materials Letters 2004;58:357-60.
[11] Hornberger H, Virtanen S, Boccaccini AR. Biomedical coatings on magnesium alloys - a review. Acta biomaterialia 2012;8:2442-55.
[12] Gray JE, Luan B. Protective coatings on magnesium and its alloys — a critical review. Journal of Alloys and Compounds 2002;336:88-113.
[13] Froats A, Aune TK, Hawke D, Unsworth W, Hillis J. Corrosion of magnesium and magnesium alloys. Metals Handbook: ASM 1987.
[14] Barfield W, G C, JD D, YH A, LA H. The potential of magnesium alloy use in orthopaedic surgery. Current Orthopaedic Practice 2012;23:146-50.
[15] Nascimento ML, Fleck C, Müller W-D. Investigation of Magnesium in NaCl 0.02 M using LSV Combined with Electrochemical Impedance Spectroscopy. ECS Transactions 2010;25:177-83.
[16] E. P. Beiträge zur Technik der Blutgefäss- und Nervennaht nebst Mittheilungen über die Verwendung eines resorbirbaren Metalles in der Chirurgie. Archiv fur klinische Chirurgie 1900:67-93.
[17] Ezechieli M, Diekmann J, Weizbauer A, Becher C, Willbold E, Helmecke P, et al. Biodegradation of a magnesium alloy implant in the intercondylar femoral notch showed an appropriate response to the synovial membrane in a rabbit model in vivo. Journal of biomaterials applications 2014.
[18] Wong HM, Yeung KW, Lam KO, Tam V, Chu PK, Luk KD, et al. A biodegradable polymer-based coating to control the performance of magnesium alloy orthopaedic implants. Biomaterials 2010;31:2084-96.
[19] Ren Y, Huang J, Zhang B, Yang K. Preliminary study of biodegradation of AZ31B magnesium alloy. Frontiers of Materials Science in China 2007;1:401-4.

[20] Kraus T, Fischerauer SF, Hanzi AC, Uggowitzer PJ, Loffler JF, Weinberg AM. Magnesium alloys for temporary implants in osteosynthesis: in vivo studies of their degradation and interaction with bone. Acta biomaterialia 2012;8:1230-8.
[21] Erdmann N, Angrisani N, Reifenrath J, Lucas A, Thorey F, Bormann D, et al. Biomechanical testing and degradation analysis of MgCa0.8 alloy screws: a comparative in vivo study in rabbits. Acta biomaterialia 2011;7:1421-8.
[22] von der Höh N, Bormann D, Lucas A, F T, Meyer-Lindenberg A. Comparison of the in vivo degradation progress of solid magnesium alloy cylinders and screw-shaped magnesium alloy cylinders in a rabbit model. Materials Science Forum 2010;638:742-7.
[23] Lensing R, Behrens P, Müller PP, Lenarz T, Stieve M. In vivo testing of a bioabsorbable magnesium alloy serving as total ossicular replacement prostheses. Journal of biomaterials applications 2014;28:688-96.
[24] Fischerauer SF, Kraus T, Wu X, Tangl S, Sorantin E, Hanzi AC, et al. In vivo degradation performance of micro-arc-oxidized magnesium implants: a micro-CT study in rats. Acta biomaterialia 2013;9:5411-20.
[25] Huehnerschulte TA, Reifenrath J, von Rechenberg B, Dziuba D, Seitz JM, Bormann D, et al. In vivo assessment of the host reactions to the biodegradation of the two novel magnesium alloys ZEK100 and AX30 in an animal model. Biomedical engineering online 2012;11:14.
[26] Zhou W, Shen T, Aung NN. Effect of heat treatment on corrosion behaviour of magnesium alloy AZ91D in simulated body fluid. Corrosion Science 2010;52:1035-41.
[27] Zhen Z, Xi T-f, Zheng Y-f. A review on in vitro corrosion performance test of biodegradable metallic materials. Transactions of Nonferrous Metals Society of China 2013;23:2283-93.
[28] Eliezer A, Witte F. Corrosion behavior of magnesium alloys in biomedical environments. Advanced Materials Research2010. p. 17-20.
[29] Liu C, Xin Y, Tian X, Chu PK. Degradation susceptibility of surgical magnesium alloy in artificial biological fluid containing albumin. Journal of Materials Research 2007;22:1806-14.
[30] Wen Z, Wu C, Dai C, Yang F. Corrosion behaviors of Mg and its alloys with different Al contents in a modified simulated body fluid. Journal of Alloys and Compounds 2009;488:392-9.
[31] Witte F, Feyerabend F, Maier P, Fischer J, Störmer M, Blawert C, et al. Biodegradable magnesium–hydroxyapatite metal matrix composites. Biomaterials 2007;28:2163-74.
[32] Yang L, Zhang E. Biocorrosion behavior of magnesium alloy in different simulated fluids for biomedical application. Materials Science and Engineering: C 2009;29:1691-6.
[33] Ghali E, Dietzel W, Kainer K-U. Testing of general and localized corrosion of magnesium alloys: A critical review. Journal of materials engineering and performance 2004;13:517-29.
[34] Lunder O, Lein JE, Hesjevik SM, Aune TK, Nişancioğlu K. Corrosion morphologies on magnesium alloy AZ 91. Materials and Corrosion 1994;45:331-40.
[35] Song G, Bowles AL, StJohn DH. Corrosion resistance of aged die cast magnesium alloy AZ91D. Materials Science and Engineering: A 2004;366:74-86.

[36] Wu G, Fan Y, Gao H, Zhai C, Zhu YP. The effect of Ca and rare earth elements on the microstructure, mechanical properties and corrosion behavior of AZ91D. Materials Science and Engineering: A 2005;408:255-63.
[37] Yan T, Tan L, Xiong D, Liu X, Zhang B, Yang K. Fluoride treatment and in vitro corrosion behavior of an AZ31B magnesium alloy. Materials Science and Engineering: C 2010;30:740-8.
[38] Ng WF, Chiu KY, Cheng FT. Effect of pH on the in vitro corrosion rate of magnesium degradable implant material. Materials Science and Engineering: C 2010;30:898-903.
[39] Chun-Yan Z, Rong-Chang Z, Cheng-Long L, Jia-Cheng G. Comparison of calcium phosphate coatings on Mg–Al and Mg–Ca alloys and their corrosion behavior in Hank's solution. Surface and Coatings Technology 2010;204:3636-40.
[40] Bender S, Goellner J, Heyn A, Boese E. Corrosion and corrosion testing of magnesium alloys. Materials and Corrosion 2007;58:977-82.
[41] Gu X, Zheng Y, Cheng Y, Zhong S, Xi T. In vitro corrosion and biocompatibility of binary magnesium alloys. Biomaterials 2009;30:484-98.
[42] Pardo A, Merino MC, Coy AE, Arrabal R, Viejo F, Matykina E. Corrosion behaviour of magnesium/aluminium alloys in 3.5 wt.% NaCl. Corrosion Science 2008;50:823-34.
[43] Scharf C, Ditze A, Shkurankov A, Morales E, Blawert C, Dietzel W, et al. Corrosion of AZ 91 Secondary Magnesium Alloy. Advanced Engineering Materials 2005;7:1134-42.
[44] Shi Z, Liu M, Atrens A. Measurement of the corrosion rate of magnesium alloys using Tafel extrapolation. Corrosion Science 2010;52:579-88.
[45] Song G, Atrens A, John DS, Wu X, Nairn J. The anodic dissolution of magnesium in chloride and sulphate solutions. Corrosion Science 1997;39:1981-2004.
[46] Song G, Atrens A, Stjohn D, Nairn J, Li Y. The electrochemical corrosion of pure magnesium in 1 N NaCl. Corrosion Science 1997;39:855-75.
[47] Huang L, Qiao D, Green BA, Liaw PK, Wang J, Pang S, et al. Bio-corrosion study on zirconium-based bulk-metallic glasses. Intermetallics 2009;17:195-9.
[48] Alvarez-Lopez M, Pereda MD, del Valle JA, Fernandez-Lorenzo M, Garcia-Alonso MC, Ruano OA, et al. Corrosion behaviour of AZ31 magnesium alloy with different grain sizes in simulated biological fluids. Acta Biomaterialia 2010;6:1763-71.
[48] Alvarez-Lopez M, Pereda MD, del Valle JA, Fernandez-Lorenzo M, Garcia-Alonso MC, Ruano OA, et al. Corrosion behaviour of AZ31 magnesium alloy with different grain sizes in simulated biological fluids. Acta Biomaterialia 2010;6:1763-71.
[49] Barranco V, Carmona N, Galván JC, Grobelny M, Kwiatkowski L, Villegas MA. Electrochemical study of tailored sol–gel thin films as pre-treatment prior to organic coating for AZ91 magnesium alloy. Progress in Organic Coatings 2010;68:347-55.
[50] op't Hoog C, Birbilis N, Estrin Y. Corrosion of Pure Mg as a Function of Grain Size and Processing Route. Advanced Engineering Materials 2008;10:579-82.
[51] Chiu KY, Wong MH, Cheng FT, Man HC. Characterization and corrosion studies of fluoride conversion coating on degradable Mg implants. Surface and Coatings Technology 2007;202:590-8.
[52] Fekry AM, El-Sherif RM. Electrochemical corrosion behavior of magnesium and titanium alloys in simulated body fluid. Electrochimica Acta 2009;54:7280-5.

[53] Gu XN, Zheng YF, Chen LJ. Influence of artificial biological fluid composition on the biocorrosion of potential orthopedic Mg-Ca, AZ31, AZ91 alloys. Biomedical materials (Bristol, England) 2009;4:065011.
[54] Hiromoto S, Yamamoto A, Maruyama N, Somekawa H, Mukai T. Polarization behavior of pure magnesium under a controlled flow in a NaCl solution. Materials Transactions 2008;49:1456-61.
[55] Kannan MB, Raman RKS. Evaluating the stress corrosion cracking susceptibility of Mg–Al–Zn alloy in modified-simulated body fluid for orthopaedic implant application. Scripta Materialia 2008;59:175-8.
[56] Müller WD, de Mele MF, Nascimento ML, Zeddies M. Degradation of magnesium and its alloys: dependence on the composition of the synthetic biological media. Journal of biomedical materials research Part A 2009;90:487-95.
[57] Müller WD, Nascimento ML, Zeddies M, Córsico M, Gassa LM, Mele MAFLd. Magnesium and its alloys as degradable biomaterials: corrosion studies using potentiodynamic and EIS electrochemical techniques. Materials Research 2007;10:5-10.
[58] Ng WF, Wong MH, Cheng FT. Stearic acid coating on magnesium for enhancing corrosion resistance in Hanks' solution. Surface and Coatings Technology 2010;204:1823-30.
[59] Peng Q, Huang Y, Zhou L, Hort N, Kainer KU. Preparation and properties of high purity Mg-Y biomaterials. Biomaterials 2010;31:398-403.
[60] Rettig R, Virtanen S. Time-dependent electrochemical characterization of the corrosion of a magnesium rare-earth alloy in simulated body fluids. Journal of Biomedical Materials Research Part A 2008;85:167-75.
[61] Song YW, Shan DY, Han EH. Electrodeposition of hydroxyapatite coating on AZ91D magnesium alloy for biomaterial application. Materials Letters 2008;62:3276-9.
[62] Südholz AD, Birbilis N, Bettles CJ, Gibson MA. Corrosion behaviour of Mg-alloy AZ91E with atypical alloying additions. Journal of Alloys and Compounds 2009;471:109-15.
[63] Wan Y, Xiong G, Luo H, He F, Huang Y, Zhou X. Preparation and characterization of a new biomedical magnesium–calcium alloy. Materials & Design 2008;29:2034-7.
[64] Xin Y, Liu C, Huo K, Tang G, Tian X, Chu PK. Corrosion behavior of ZrN/Zr coated biomedical AZ91 magnesium alloy. Surface and Coatings Technology 2009;203:2554-7.
[65] Wan YZ, Xiong GY, Luo HL, He F, Huang Y, Wang YL. Influence of zinc ion implantation on surface nanomechanical performance and corrosion resistance of biomedical magnesium-calcium alloys. Applied Surface Science 2008;254:5514-6.
[66] Xu L, Zhang E, Yang K. Phosphating treatment and corrosion properties of Mg-Mn-Zn alloy for biomedical application. Journal of Materials Science: Materials in Medicine 2009;20:859-67.
[67] Zhang E, Yin D, Xu L, Yang L, Yang K. Microstructure, mechanical and corrosion properties and biocompatibility of Mg-Zn-Mn alloys for biomedical application. Materials Science and Engineering C 2009;29:987-93.
[68] Kannan MB, Raman RKS. In vitro degradation and mechanical integrity of calcium-containing magnesium alloys in modified-simulated body fluid. Biomaterials 2008;29:2306-14.

[69] Zhang S, Zhang X, Zhao C, Li J, Song Y, Xie C, et al. Research on an Mg-Zn alloy as a degradable biomaterial. Acta Biomaterialia 2010;6:626-40.
[70] Xin Y, Liu C, Zhang X, Tang G, Tian X, Chu PK. Corrosion behavior of biomedical AZ91 magnesium alloy in simulated body fluids. Journal of Materials Research 2007;22:2004-11.
[71] Wang H, Estrin Y, Fu H, Song G, Zúberová Z. The Effect of Pre-Processing and Grain Structure on the Bio-Corrosion and Fatigue Resistance of Magnesium Alloy AZ31. Advanced Engineering Materials 2007;9:967-72.
[72] Wang H, Shi ZM, Yang K. Magnesium and magnesium alloys as degradable metallic biomaterials. Advanced Materials Research2008. p. 207-10.
[73] Yun Y, Dong Z, Yang D, Schulz MJ, Shanov VN, Yarmolenko S, et al. Biodegradable Mg corrosion and osteoblast cell culture studies. Materials Science and Engineering: C 2009;29:1814-21.
[74] Chang JW, Guo XW, Fu PH, Peng LM, Ding WJ. Effect of heat treatment on corrosion and electrochemical behaviour of Mg-3Nd-0.2Zn-0.4Zr (wt.%) alloy. Electrochimica Acta 2007;52:3160-7.
[75] Liu CL, Wang YJ, Zeng RC, Zhang XM, Huang WJ, Chu PK. In vitro corrosion degradation behaviour of Mg–Ca alloy in the presence of albumin. Corrosion Science 2010;52:3341-7.
[76] Song G, Song S. A Possible Biodegradable Magnesium Implant Material. Advanced Engineering Materials 2007;9:298-302.
[77] Contu F, Elsener B, Böhni H. Characterization of implant materials in fetal bovine serum and sodium sulfate by electrochemical impedance spectroscopy. II. Coarsely sandblasted samples. Journal of Biomedical Materials Research Part A 2003;67:246-54.
[78] Gunde P, Furrer A, Hänzi AC, Schmutz P, Uggowitzer PJ. The influence of heat treatment and plastic deformation on the bio-degradation of a Mg-Y-RE alloy. Journal of Biomedical Materials Research Part A 2010;92:409-18.
[79] Kuwahara H, Al-Abdullat Y, Mazaki N, Tsutsumi S, Aizawa T. Precipitation of magnesium apatite on pure magnesium surface during immersing in Hank's solution. Materials Transactions 2001;42:1317-21.
[80] Quach NC, Uggowitzer PJ, Schmutz P. Corrosion behaviour of an Mg-Y-RE alloy used in biomedical applications studied by electrochemical techniques. Comptes Rendus Chimie 2008;11:1043-54.
[81] Shi P, Ng WF, Wong MH, Cheng FT. Improvement of corrosion resistance of pure magnesium in Hanks' solution by microarc oxidation with sol-gel TiO2 sealing. Journal of Alloys and Compounds 2009;469:286-92.
[82] Wang H, Akid R, Gobara M. Scratch-resistant anticorrosion sol–gel coating for the protection of AZ31 magnesium alloy via a low temperature sol–gel route. Corrosion Science 2010;52:2565-70.
[83] Kirkland NT, Birbilis N, Staiger MP. Assessing the corrosion of biodegradable magnesium implants: a critical review of current methodologies and their limitations. Acta biomaterialia 2012;8:925-36.
[84] Zhang S, Zhang X, Zhao C, Li J, Song Y, Xie C, et al. Research on an Mg–Zn alloy as a degradable biomaterial. Acta biomaterialia 2010;6:626-40.

[85] Witte F, Fischer J, Nellesen J, Crostack HA, Kaese V, Pisch A, et al. In vitro and in vivo corrosion measurements of magnesium alloys. Biomaterials 2006;27:1013-8.
[86] Seitz J-M, Collier K, Wulf E, Bormann D, Bach F-W. Comparison of the Corrosion Behavior of Coated and Uncoated Magnesium Alloys in an In Vitro Corrosion Environment. Advanced Engineering Materials 2011;13:B313-B23.
[87] Jo JH, Kang BG, Shin KS, Kim HE, Hahn BD, Park DS, et al. Hydroxyapatite coating on magnesium with MgF(2) interlayer for enhanced corrosion resistance and biocompatibility. Journal of materials science Materials in medicine 2011;22:2437-47.
[88] Li Z, Gu X, Lou S, Zheng Y. The development of binary Mg-Ca alloys for use as biodegradable materials within bone. Biomaterials 2008;29:1329-44.
[89] Schinhammer M, Steiger P, Moszner F, Loffler JF, Uggowitzer PJ. Degradation performance of biodegradable Fe-Mn-C(-Pd) alloys. Materials science & engineering C, Materials for biological applications 2013;33:1882-93.
[90] Xu L, Yu G, Zhang E, Pan F, Yang K. In vivo corrosion behavior of Mg-Mn-Zn alloy for bone implant application. Journal of biomedical materials research Part A 2007;83:703-11.
[91] Carboneras M, Pérez-Maceda BT, Valle Jd, García-Alonso MC, Alobera MA, Clemente C, et al. Comportamiento frente a la corrosión y biocompatibilidad in vitro/in vivo de la aleación AZ31 modificada superficialmente. Revista de Metalurgia 2011;47:212-23.
[92] Wang J, Tang J, Zhang P, Li Y, Wang J, Lai Y, et al. Surface modification of magnesium alloys developed for bioabsorbable orthopedic implants: A general review. Journal of biomedical materials research Part B, Applied biomaterials 2012;100B:1691-701.
[93] Wang H, Shi Z. In vitro biodegradation behavior of magnesium and magnesium alloy. Journal of biomedical materials research Part B, Applied biomaterials 2011;98:203-9.
[94] Witte F, Kaese V, Haferkamp H, Switzer E, Meyer-Lindenberg A, Wirth CJ, et al. In vivo corrosion of four magnesium alloys and the associated bone response. Biomaterials 2005;26:3557-63.
[95] Li Z, Song G-L, Song S. Effect of bicarbonate on biodegradation behaviour of pure magnesium in a simulated body fluid. Electrochimica Acta 2014;115:56-65.
[96] Salahshoor M, Guo Y. Biodegradable Orthopedic Magnesium-Calcium (MgCa) Alloys, Processing, and Corrosion Performance. Materials 2012;5:135-55.
[97] Yang JX, Cui FZ, Lee IS, Zhang Y, Yin QS, Xia H, et al. In vivo biocompatibility and degradation behavior of Mg alloy coated by calcium phosphate in a rabbit model. Journal of biomaterials applications 2012;27:153-64.
[98] Willumeit R, Feyerabend F, Huber N. Magnesium degradation as determined by artificial neural networks. Acta biomaterialia 2013;9:8722-9.
[99] Staiger MP, Pietak AM, Huadmai J, Dias G. Magnesium and its alloys as orthopedic biomaterials: A review. Biomaterials 2006;27:1728-34.
[100] Chai H, Guo L, Wang X, Gao X, Liu K, Fu Y, et al. In vitro and in vivo evaluations on osteogenesis and biodegradability of a beta-tricalcium phosphate coated magnesium alloy. Journal of biomedical materials research Part A 2011.

[101] Yang L, Hort N, Willumeit R, Feyerabend F. Effects of corrosion environment and proteins on magnesium corrosion. Corrosion Engineering Science and Technology 2012;47:335-9.
[102] Kirkland NT, Birbilis N, Walker J, Woodfield T, Dias GJ, Staiger MP. In-vitro dissolution of magnesium-calcium binary alloys: clarifying the unique role of calcium additions in bioresorbable magnesium implant alloys. Journal of biomedical materials research Part B, Applied biomaterials 2010;95:91-100.
[103] Yamamoto A, Hiromoto S. Effect of inorganic salts, amino acids and proteins on the degradation of pure magnesium in vitro. Materials Science and Engineering: C 2009;29:1559-68.
[104] Walker J, Shadanbaz S, Kirkland NT, Stace E, Woodfield T, Staiger MP, et al. Magnesium alloys: predicting in vivo corrosion with in vitro immersion testing. Journal of biomedical materials research Part B, Applied biomaterials 2012;100:1134-41.
[105] Kirkland NT, Waterman J, Birbilis N, Dias G, Woodfield TB, Hartshorn RM, et al. Buffer-regulated biocorrosion of pure magnesium. Journal of materials science Materials in medicine 2012;23:283-91.
[106] Rettig R, Virtanen S. Composition of corrosion layers on a magnesium rare-earth alloy in simulated body fluids. Journal of biomedical materials research Part A 2009;88:359-69.
[107] Schinhammer M, Hofstetter J, Wegmann C, Moszner F, Löffler JF, Uggowitzer PJ. On the Immersion Testing of Degradable Implant Materials in Simulated Body Fluid: Active pH Regulation Using CO2. Advanced Engineering Materials 2013;15:434-41.
[108] Kokubo T, Takadama H. How useful is SBF in predicting in vivo bone bioactivity? Biomaterials 2006;27:2907-15.
[109] Willumeit R, Fischer J, Feyerabend F, Hort N, Bismayer U, Heidrich S, et al. Chemical surface alteration of biodegradable magnesium exposed to corrosion media. Acta biomaterialia 2011;7:2704-15.
[110] Merritt K, Brown SA, Sharkey NA. The binding of metal salts and corrosion products to cells and proteins in vitro. Journal of biomedical materials research 1984;18:1005-15.
[111] Clark GC, Williams DF. The effects of proteins on metallic corrosion. Journal of biomedical materials research 1982;16:125-34.
[112] Liu C. Degradation susceptibility of surgical magnesium alloy in artificial biological fluid containing albumin. J Mater Res 2007;22:1806-18014.
[113] Witte F, Hort N, Vogt C, Cohen S, Kainer KU, Willumeit R, et al. Degradable biomaterials based on magnesium corrosion. Current Opinion in Solid State and Materials Science 2008;12:63-72.
[114] Seyfarth H. [Problem of implantation of foreign bodies]. Archiv fur orthopadische und Unfall-Chirurgie 1956;48:254-69.
[115] Badawy WA, Hilal NH, El-Rabiee M, Nady H. Electrochemical behavior of Mg and some Mg alloys in aqueous solutions of different pH. Electrochimica Acta 2010;55:1880-7.
[116] Erdmann N, Bondarenko A, Hewicker-Trautwein M, Angrisani N, Reifenrath J, Lucas A, et al. Evaluation of the soft tissue biocompatibility of MgCa0.8 and surgical steel 316L in vivo: a comparative study in rabbits. Biomedical engineering online 2010;9:63.

[117] Zainal Abidin NI, Rolfe B, Owen H, Malisano J, Martin D, Hofstetter J, et al. The in vivo and in vitro corrosion of high-purity magnesium and magnesium alloys WZ21 and AZ91. Corrosion Science 2013;75:354-66.

Fig. 1: Comparison of the averaged *in vitro* and *in vivo* corrosion rates of 20 different materials.

Fig. 2: Corrosion factors *in vitro-in vivo,* same order as in Fig. 1.

Fig. 3: Corrosion factors grouped regarding the medium employed for *in vitro* testing.

Figure 1

Click here to download high resolution image

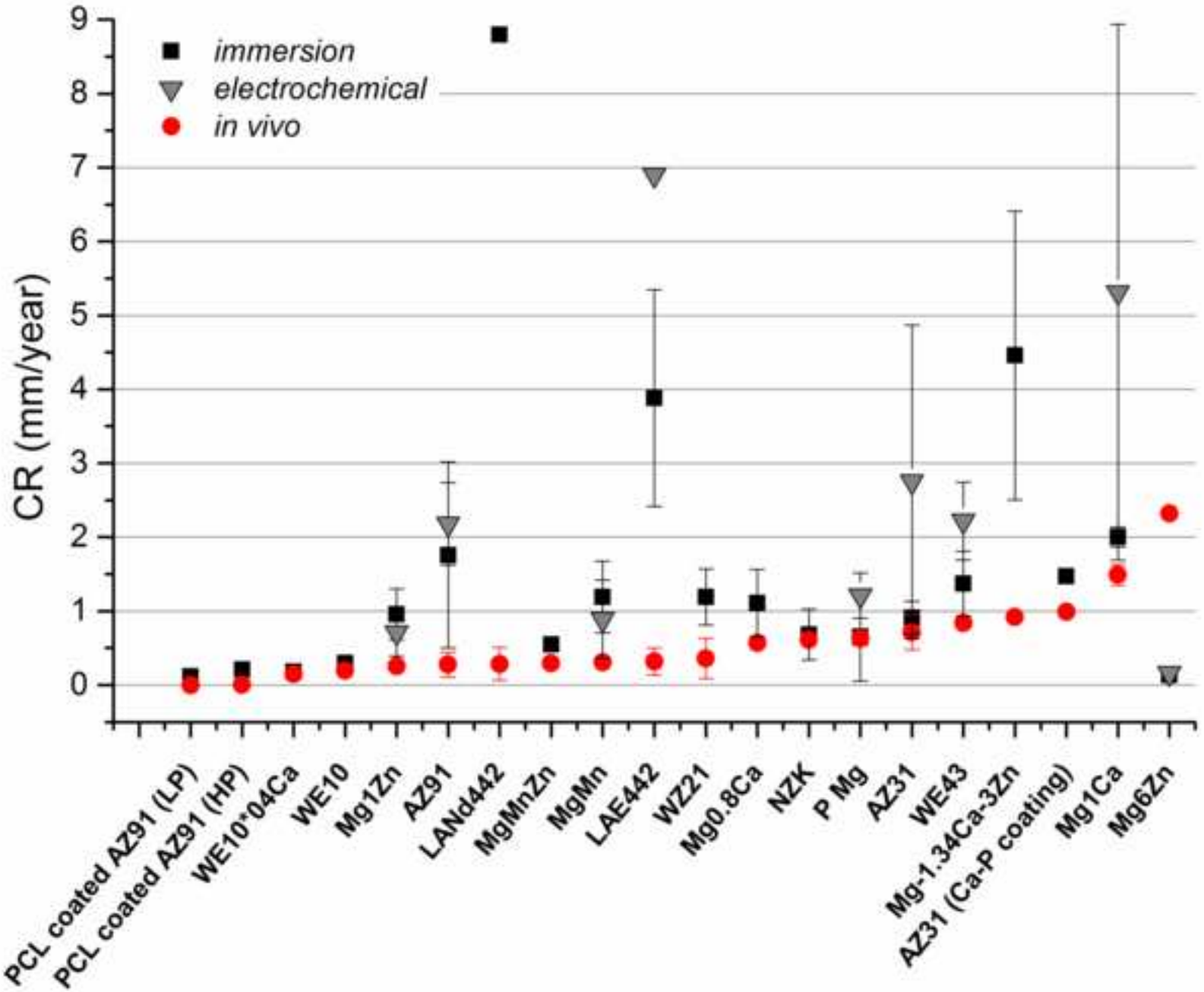

Figure 2

Click here to download high resolution image

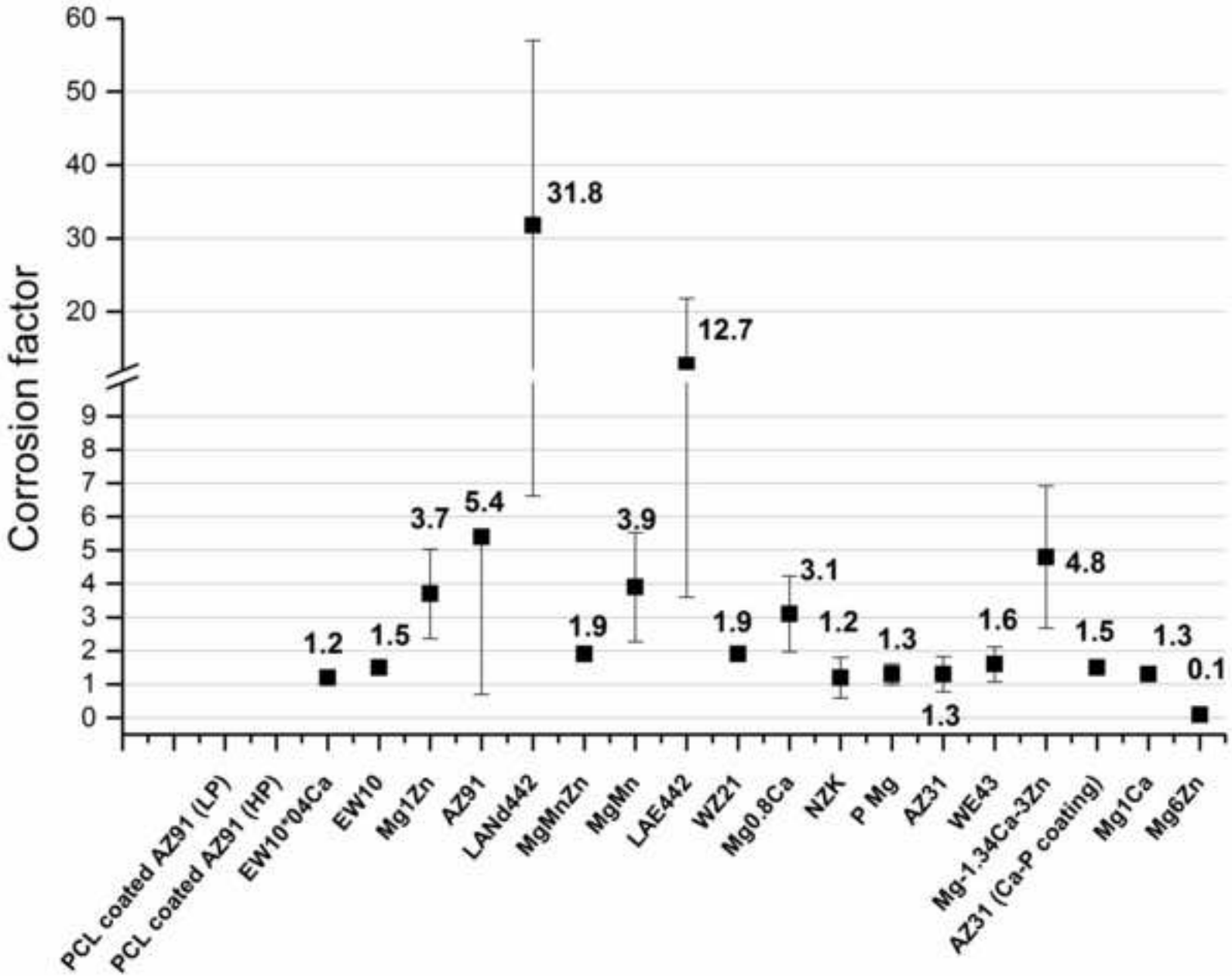

Figure 3

Click here to download high resolution image

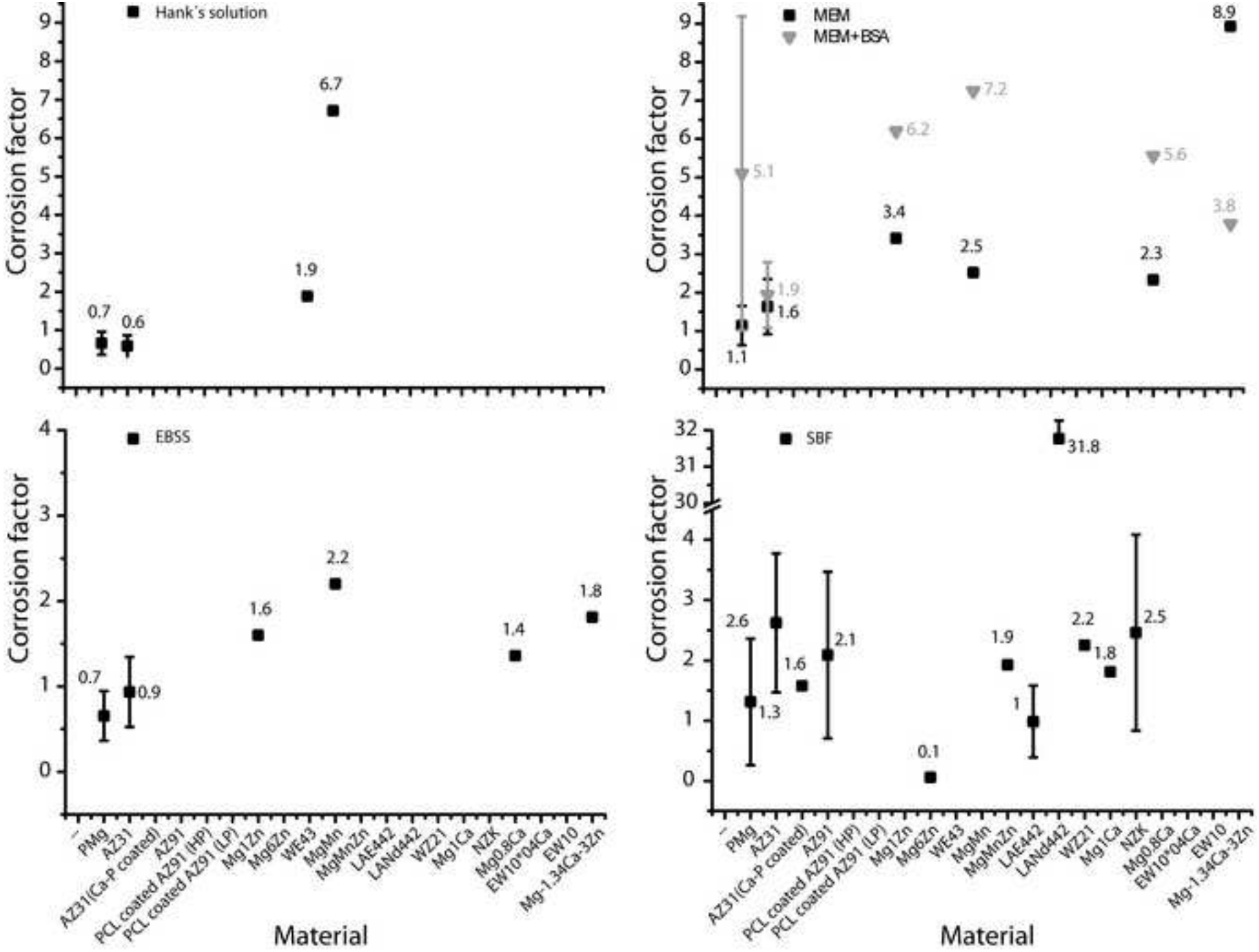

Table(s)

Table 1: Summary of the corrosion rates *in vivo*. (* no corrosion rate *in vitro* available)

Material name	Material composition (wt%)	Days of evaluation	Corrosion rate In mm/year (unless otherwise indicated)	Method	Animal model	Implantation side	Average corrosion rate (mm/year)	Ref
PMg	>99% Mg	7	0.39	weight loss	rat	subcutaneous (dorsal abdominal region)	0.33	[1]
		14	0.39					
		21	0.221					
		0	0.001733±0.000153 g	weight loss	rat	femur (not intramedullary)	0.86	[2]
		30	0.00105±7.07E-05 g					
		60	0.64	weight loss	rat	intramuscular (lower back)	0.64	[3]
AZ31 (Ca-P coating)	*Mg- 3.37% Al, 0.78% Zn, 0.22% Mn, 0.0134% Si, 0.001% Cu, 0.002% Ni, 0.0027% Fe*	56	32 mm^2(remaining volume)	volume reduction	rabbit	femur (not intramedullary)	0.99	[4]
AZ31		56	24 mm^2(remaining volume)		rabbit	femur (not intramedullary)	1.64	
		42	1.6 mm^2	area reduction	guinea pig	femur (intramedullary)	0.4 mm^2/12 weeks	[5]
		126	1.2 mm^2					
AZ31 (βTCP coating)*		84	17%	% of area reduction	rat	femur (not intramedullary)	0.168	[6]
AZ31		84	33%	% of area reduction	rat	femur (not intramedullary)	0.326	
AZ31		7	0.335	weight loss	rat	subcutaneous (dorsal abdominal region)	0.3	[1]
		14	0.335					
		21	0.223					
AZ31		42	1.17 mg/mm^2/year	area reduction	guinea pig	femur (intramedullary)	3.2	[7]
		126						
AZ91	Mg- 9% Al, 1% Zn HP Coating: 2.2% Polycaprolactone (PCL) LP Coating: 3.33% PCL	60	0.56	weight loss	rat	Intramuscular (lower back)	0.56	[3]
AZ91		60	0.33%	% of volume reduction	rabbit	femur trocanter (not intramedullary)	0.013	[8]
PCL coated AZ91(HP)		60	0.05%				0.002	
PCL coated AZ91(LP)		60	0%				0	
AZ91D		126	0.0003516	volume reduction	guinea pig	femur (intramedullary)	0.0003516	[9]
		estimated					0.76	[7]
AZ91		42	1.6 mm^2	area reduction	guinea pig	femur (intramedullary)	0.5 mm^2/12 weeks	[5]
		126	1.1 mm^2					
		estimated					0	[10]
WE43	Mg- 4.16% Y, 0.36% Zr, 0.20% Zn, 0.13% Mn, 3.80% RE: 71%Nd, 8%Ce, 8%Dy, 6%La	42	1.1 mm^2	area reduction	guinea pig	femur (intramedullary)	0.7 mm^2/12 weeks	[5]
		126	1.8 mm^2					
		estimated					4.13	[7]
Mg1Zn	Mg- 1% Zn	7	0.378	weight loss	rat	subcutaneous (dorsal abdominal region)	0.26	[1]
		14	0.227					
		21	0.164					
MgMn	Mg- 1% Mn	7	0.302	weight loss	rat	subcutaneous (dorsal abdominal region)	0.298	
		14	0.34					
		21	0.252					
MgMnZn	Mg- 1.2% Mn, 1% Zn	63	10-17% Mg degraded (0.19 mm/year)	area reduction	rat	femur (intramedullary)	0.286	[11]
		126	54% Mg degraded (0.38 mm/year)					
Mg6Zn	Mg- 6% Zn	94	2.32±0.11	% of weight loss	rabbit	femur (intramedullary)	2.32	[12]
ZX50*	Mg- 5% Zn, 0.25% Ca, 0.15% Mn	84	1.2% of volume reduction /day	% of volume reduction	rat	femur (mid-diaphyseal region; not intramedullary)	1.58	[13]
		7	1.7% of volume reduction /day	volume reduction	rat	femur (mid-diaphyseal region; not intramedullary)	2.3	[14]
		14	1.7% of volume reduction /day					
		21	1.7% of volume reduction /day					
		28	1.7% of volume reduction /day					
		56	3% of volume reduction /day					
		84	4% of volume reduction /day					
WZ21	Mg- 2% Y, 1% Zn, 0.25% Ca, 0.15% Mn	84	0.3% of volume reduction/ day	% of volume reduction	rat	femur (mid-diaphyseal region; not intramedullary)	0.36	[13]
		168	0.5% of volume reduction /day					
		60	0.91	weight loss	rat	intramuscular (lower back)	0.91	[3]
LAE442	Mg- 4% Li, 4% Al, 2.2% Se, 0.2% Mn; RE: 51% Ce, 22% La, 16% Nd, 8% Pr	42	1.7 mm^2	area reduction	guinea pig	femur (intramedullary)	0.15 mm^2/12weeks	[5]
		126	1.5 mm^2					
		estimated					74.51 mm^3/year	[7]
		126	$1.205*10^{-4}$	volume reduction	guinea pig	femur (intramedullary)	$1.205*10^{-4}$	[9]
		14	0.58	volume reduction	rabbit	medial femur condyle (not intramedullary)	0.445	[15]
		28	0.46					
		49	0.43					
		84	0.31					
LANd442	Mg- 4% Li, 4% Al, 2% Nd (as a single RE element)	28	0.01	volume reduction	rabbit	tibiae (intramedullary)	0.054	[16]
		56	0.02					

		91	0.03					
		182	0.072					
		182 (daily evaluation)		semiquantification of structure loss	rabbit	tibiae (intramedullary)		[17]
ZEK100*	Mg- 0.96% Zn, 0.21%Zr, 0.3% RE	60	0.067	volume reduction	rabbit	tibiae (intramedullary)	0.1105 (6 months)	[18]
		180	0.154					
		60	0.078	area and volume reduction	rabbit	tibiae (intramedullary)	0.49	[19]
		180	0.162					
		270	1.14					
		360	0.582					
NZK	Mg- 2.5% Nd, 0.2% Zn, 0.5% Zr	28	0.66 ± 0.15	weight loss	rabbit	femur (not intramedullary)	0.57	[20]
		56	0.48 ± 0.08					
EW10*04Ca	Mg- 1.2% Nd, 0.5% Y, 0.5% Zr, 0.4% Ca	42	0.16	volume reduction	rat	subcutaneous (between the scapulas and in the mid-lumbar area)	0.15	[21]
		84	0.14					
EW10	Mg- 1.2% Nd, 0.5%Y, 0.5%Zr	42	0.23	volume reduction	rat	subcutaneous (between the scapulas and in the mid-lumbar area)	0.195	
		84	0.16					
Mg1Ca	Mg- 1% Ca	30	0.04 g	weight loss	rabbit	femur (intramedullary)	2.28 mg/mm^2/year	[7]
		60	0.3 g					
		90	0.6 g					
		estimated					1.27	[22]
Mg0.8Ca	Mg- 0.8% Ca	7	0.312	weight loss	rat	subcutaneous (dorsal abdominal region)	0.36	[1]
		14	0.43					
		21	0.351					
Mg-1.34Ca-3Zn	Mg- 1.34% Ca, 3% Zn	7	0.786	weight loss	rat	subcutaneous (dorsal abdominal region)	0.92	[1]
		14	1.001					
		21	1.001					
AX30*	Mg- 3%Al, <1%Ca, 0% RE	60	0.065	volume reduction	rabbit	tibiae (intramedullary)	0.0875 (8 months)	[18]
		180	0.11					

Table 2: Methodology for evaluating the corrosion rate *in vitro, ex vivo* and *in vivo.*

in vitro					***ex vivo***		***in vivo***	
Immersion test			Electrochemical test			μCT	μCT	X-ray spectroscopy
Mass loss	Hydrogen evolution	Ion release	Potentiodynamic polarisation	Electrochemical impedance spectroscopy	Mass loss	Volume loss	Volume loss	
$CR = 8.76*10^4 \Delta W/Atρ$	$PV = nRT$	$CR = cV/St$	$CR = K(I_{corr}/ρ)m_e$		$CR = 8.76*10^4 \Delta W/Atρ$	$CR = 8.76*10^4 \Delta V/At$	$CR = 8.76*10^4 \Delta V/At$	
ΔW: weight loss A: original surface area t: exposure time $ρ$: standard density of the material	P: standard atmospheric pressure (Pa), V: volume of H_2 (m^3) n: substance amount of the gas(mol) T: temperature (K)	c: ion release concentration V: volume of immersion solution S: original surface area exposed to corrosive media t: exposure time	K: 3.273×10^{-3} mm·g/(μA·cm·a) I_{corr}: is the current density m_e: equivalent mass.		ΔW: weight loss A: original surface area t: exposure time $ρ$: standard density of the material	ΔV: differences in volume before-after immersion A: original surface area t: exposure time		

Table 3: Summary of the corrosion rates *in vitro.*

Material name	Days of evaluation	Corrosion rate in mm/year (unless otherwise indicated)	Specified parameters	Test	Solution	Average corrosion rate (mm/year)	Ref.
PMg	7	0.572		immersion	EBSS	0.39	[1]
	14	0.468					
	21	0.382					
	7	0.728			MEM	0.68	
	14	0.676					
	21	0.659					
	7	2.185			MEM + BSA	1.68	
	14	1.483					
	21	1.370					
	5	0.2 mg/cm^2 (0.04 mm/year)		immersion	0.9% NaCl solution	0.5	[23]
	10	2 mg/cm^2(0.4 mm/year)	37ºC				
	20	5.1 mg/cm^2(1.07 mm/year)					
		0.3 mg/cm^2/day		immersion	McCoy´s 5A-5%FBS	0.15	[7]
	3	0.43±0.04		immersion	SBF (0.68%NaCl)	0.26	[12]
	30	0.10±0.07					
				electrochemical		0.2	
	5	2.25	dynamic test	immersion	Hank´s solution (0.8% NaCl)	1.52	[24]
	5-20	0.8					
	5	0.6	static test			0.42	
	5-20	0.25					
	3	2.50±0.54		immersion	SBF	1.3	[25]
	7	1.33±0.23					
	30	0.40±0.06					
	7	3.22		immersion	Notr´s solution (CO_2 – bicarbonate buffered Hank's solution)	2.05	[3]
	14	0.88					
				electrochemical	Hank´s solution	0.36	[7]
		1.14		electrochemical	1N NaCL	1.14	[26]
		2.7		electrochemical	1M NaCl	2.7	[27]
		1.94	as-cast	electrochemical	SBF	1.39	[28]
		0.84	as-rolled				
		0.36	as-cast		Hank´s solution	0.29	
		0.22	as-rolled				
	16	0.686		electrochemical	m-SBF	2.523	[29]
	24	1.837					
AZ31B	2	1.1		immersion	Hank´s solution	0.3	[30]
	5	0.9					
	10	0.3					
	20	0.5					
	30	0.75					
AZ31	16	0.735		electrochemical	m-SBF	0.628	[29]
	24	0.521					
		6.99		electrochemical	3.5% NaCl	6.99	[31]
AZ31 (Ca-P coating)	56	7 mg/day		immersion	SBF (0.8% NaCl)	1.47	[32]
	56	9 mg/day		immersion		1.88	
AZ31	7	0.795		immersion	EBSS	0.67	[1]
	14	0.670					
	21	0.546					
	7	1.291			MEM	1.167	
	14	1.018					
	21	1.192					
	7	1.937			MEM + BSA	1.39	
	14	1.291					
	21	0.944					
	1	0.766	squeeze casting	immersion	Hank´s solution (0.8% NaCl)	0.5355	[33]
	2	0.694					
	5	0.584					
	10	0.475					
	15	0.365					
	20	0.329					
	1	0.545	hot rolling			0.48	
	2	0.475					
	5	0.438					
	10	0.365					
	15	0.329					
	20	0.255					
	5	2.25	dynamic test	immersion	Hank´s solution (0.8% NaCl)	0.25	[24]
	5-20	0.8					
	5	0.6				1.52	
	5-20	0.25					
		Weight loss / ***Release of Mg ions***					
AZ91	5	/ 0.05		immersion	SBF	0.56	[8]

	15		0.012					
	30		0.014					
	60	17 mg	0.017					
PCL coated AZ91 (HP)	5		0.001				0.21	
	15		0.0025					
	30		0.0025					
	60	6.22	0.006					
PCL coated AZ91 (LP)	5		0.001				0.12	
	15		0.0015					
	30		0.0025					
	60	3.59	0.004					
AZ91	7	6.23			immersion	Notr´s solution (CO_2 – bicarbonate buffered Hank's solution)	6.23	[3]
AZ91D	10	-0.267			immersion	solution of 25 L containing NaCl (710 g). $MgSO_4$ (205 g). $MgCl_2$ $6H_2O$ (107.5 g). $CaCl_2$ $6H_2O$ (50 g)	0	[9]
					electrochemical		2.8	
						modified SBF+HEPES (pH7.4)	1.1	[34]
		5.72			electrochemical	1N NaCL	5.72	[26]
		0.66				1N NaCL	0.66	
		0.91			electrochemical	1M NaCl	0.91	[27]
		2.93			electrochemical	2.3% NaCl	2.93	[35]
		0.85		as cast	electrochemical	SBF	0.72	[36]
		0.61		heat treated (T4)				
	16	2.583			electrochemical	m-SBF	2.83	[29]
	24	3.076						
		2.21			electrochemical	3.5% NaCl	2.21	[31]
WE43	26	1.58			immersion	Hank´s solution	1.58	[37]
	126	0.0025			immersion	solution of 25 L containing NaCl (710 g). $MgSO_4$ (205 g). $MgCl_2$ $6H_2O$ (107.5 g). $CaCl_2$ $6H_2O$ (50 g)	0.0025	[9]
	10	2.2			immersion	Hank´s solution	2.2	[38]
		0.64			electrochemical	0.1 M NaCl	2.22	[8]
		1.63				0.2 M NaCl		
		2.51				0.6 M NaCl		
		2.97				1 M NaCl		
		3.66				2 M NaCl		
Mg1Zn	7	0.505			immersion	EBSS	0.412	[1]
	14	0.429						
	21	0.303						
	7	0.959				MEM	0.872	
	14	0.833						
	21	0.824						
	7	1.716				MEM + BSA	1.59	
	14	1.438						
	21	1.615						
		1.52		as-cast	electrochemical	SBF	1.22	[28]
		0.92		as-rolled				
		0.24		as-cast		Hank´s solution	0.21	
		0.17		as-rolled				
MgMn	7	0.756			immersion	EBSS	0.66	[1]
	14	0.504						
	21	0.722						
	7	0.856				MEM	0.75	
	14	0.882						
	21	0.504						
	7	2.771				MEM + BSA	2.16	
	14	2.116						
	21	2.884						
		2.46		as-cast	electrochemical	SBF	1.46	[28]
		0.45		as-rolled				
		0.55		as-cast		Hank´s solution	0.34	
		0.13		as-rolled				
MgMnZn	126	0.55			immersion	SBF	0.55	[39]
Mg6Zn	3	0.20±0.05			immersion	SBF (0.68% NaCl)	0.135	[12]
	30	0.07±0.02						
		0.16			electrochemical		0.16	
ZX50								
WZ21	7	0.4 mg/cm^2 day			immersion	SBF (pH regulated with CO_2)	0.81	[40]
	14	0.22 mg/cm^2 day						
	21	0.2 mg/cm^2 day						
	7	0.46			immersion	Notr´s solution (CO_2 – bicarbonate buffered Hank's solution)	1.58	[3]
	14	2.7						
LAE442	10	5.535			immersion	solution of 25 L containing NaCl (710 g). $MgSO_4$ (205 g). $MgCl_2$ $6H_2O$ (107.5 g). $CaCl_2$ $6H_2O$ (50 g)	5.535	[9]
					electrochemical		6.9	
LANd442	every 24 hours until a	variation from 2.6 to 15.0 mm/year		dynamic test	immersion	SBF	8.8	[41]

	total of 25						
NZK	10	0.34		immersion	artificial plasma (AP)	0.34	[42]
	3	1.5		immersion	simulated body fluid (0.68% NaCl)	1.3	[25]
	7	1.4					
	30	0.2					
NZK-MgF2	10	0.25		immersion		0.25	[42]
EW10*04Ca	1	0.25		immersion	0.9% NaCl solution saturated with $Mg(OH)_2$ (to eliminate the effect of the corrosive products on the corrosiveness of the solution)	0.18	[43]
	2	0.33					
	3	0.28					
	4	0.25					
	5	0.21					
EW10	1	0.51				0.3	
	2	0.45					
	3	0.42					
	4	0.43					
	5	0.41					
Mg-1Ca	10	12.56	as-cast	electrochemical	SBF	12.56	[22]
		0.136 ml/cm^2/h		immersion			
		1.63	as-rolled	electrochemical		1.63	
		1.74	as-extruded	electrochemical		1.74	
		0.040 ml/cm^2/h		immersion			
Mg0.8Ca	7	0.505		immersion	EBSS	0.49	[1]
	14	0.429					
	21	0.303					
	7	0.959			MEM	0.84	
	14	0.833					
	21	0.824					
	7	1.716			MEM + BSA	2	
	14	1.438					
	21	1.615					
Mg-1.34Ca-3Zn	7	0.786		immersion	EBSS	1.668	[1]
	14	1.001					
	21	1.001					
	7	4.718			MEM	8.22	
	14	9.889					
	21	10.004					
	7	3.288			MEM + BSA	3.49	
	14	4.337					
	21	2.844					

Table 4: Example of the variation in *in vitro* corrosion rates depending on the applied methodologies.

Material	Corrosion rate *in vitro* (mm/year)	
	Electrochemical measurement	***Immersion test***
LAE442 [9]	6.90	5.53
AZ91D [9]	2.80	-0.26
Mg [12]	0.20	0.43
Mg6Zn [12]	0.16	0.20

Table 5: List of materials (PMg and Mg alloys) considered for calculation of the corrosion factors.

Material name	Material composition (wt%)	Average corrosion rate *in vitro*	Average corrosion rate *in vivo*	Reference *in vitro*	Reference *in vivo*
PMg	>99%Mg	0.65	0.63	[1. 7. 12. 25. 44]	[1. 2]
AZ31	Mg- 3.37%Al. 0.78%Zn. 0.22% Mn 0.0134% Si. 0.001% Cu. 0.002% Ni.0.0027% Fe	0.91	0.72	[24. 30. 32]	[1. 5. 6]
AZ31 (Ca-P coating)	Mg-3.37%Al. 0.78%Zn. 0.22%Mn	1.47	0.99	[32]	[4]
AZ91	Mg- 9% Al. 1%Zn	1.76	0.28	[7-9. 45. 46]	[5. 8. 9. 47]
PCL-coated AZ91 (HP)	Mg-9%Al. 1%Zn Coating: 2.2%Polycaprolactone (PCL)	0.21	0.002	[8]	[8]
PCL-coated AZ91 (LP)	Mg- 9%Al. 1%Zn Coating: 3.33%PCL	0.12	0	[8]	[8]
Mg1Zn	Mg-1%Zn	0.96	0.26	[1]	[1]
Mg6Zn	Mg- 6%Zn	0.14	2.32	[12]	[12]
WE43	Mg-4.16%Y.0.36%Zr. 0.20%Zn. 0.13%Mn3.80% RE: 71%Nd. 8%Ce. 8%Dy. 6%La	1.37	0.84	[38]	[5]
MgMn	Mg-1%Mn	1.19	0.30	[1]	[1]
MgMnZn	Mg- 1.2%Mn. 1%Zn	0.55	0.30	[11. 39]	[11]
LAE442	Mg-4%Li. 4%Al. 2.2%Se. 0.2%Mn; RE: 51%Ce. 22%La. 16%Nd.8%Pr	3.88	0.32	[9. 48]	[5. 9. 15. 49]
LANd442	Mg- 4%Li. 4%Al. 2%Nd (as a single RE element)	8.8	0.29	[17. 41]	[16. 17]
WZ21	Mg-2%Y. 1%Zn. 0.25%Ca. 0.15%Mn	1.19	0.36	[40]	[13]
NZK	Mg- 2.5%Nd. 0.2%Zn. 0.5%Zr	0.69	0.61	[25. 42]	[20]
Mg1Ca	Mg-1%Ca	2.02	1.49	[7. 22]	[22]
Mg0.8Ca	Mg-0.8%Ca	1.11	0.57	[1]	[1]
EW10*04Ca	Mg–1.2%Nd. 0.5%Y. 0.5%Zr. 0.4%Ca	0.18	0.15	[43]	[21]
EW10	Mg–1.2%Nd. 0.5%Y. 0.5%Zr	0.3	0.20	[43]	[21]
Mg-1.34Ca-3Zn	Mg-1.34%Ca. 3%Zn	4.46	0.92	[1]	[1]

Table 6: Composition of some of the commonly employed solutions for corrosion testing and blood plasma. All the concentrations are given in mMol/L unless other units are specified.

		Blood Plasma [1. 50]	Hank´s solution [3]	SBF [51]	EBSS [1]	MEM [1]
Inorganic ions	Na	142.0	142.0	142.0	144.0	143.0
	K	5.0	5.8	5.8	5.4	5.4
	Mg	1.5	0.8	1.5	0.4	0.4
	Cl	103.0	145.0	147.8	125.0	125.0
	Ca	2.5	2.5	2.5	1.8	1.8
	HPO_4	1.0	0.4	1.0	1.0	0.9
	SO_4	0.5	0.8	0.5	0.4	0.4
	HCO_3	27.0	4.2	27.0	26.0	26.0
Organic components	Glucose	3.6-5.2			5.60	5.60
	Albumin (g/L)	35-50				
	Amino acids (g/L)	Variable				0.95
	Vitamins (g/L)	Variable				8.10

References

[1] Walker J. Shadanbaz S. Kirkland NT. Stace E. Woodfield T. Staiger MP. et al. Magnesium alloys: predicting in vivo corrosion with in vitro immersion testing. Journal of biomedical materials research Part B. Applied biomaterials 2012;100:1134-41.
[2] Yang W. Zhang Y. Yang J. Tan L. Yang K. Potential antiosteoporosis effect of biodegradable magnesium implanted in STZ-induced diabetic rats. Journal of biomedical materials research Part A 2011;99:386-94.
[3] Zainal Abidin NI. Rolfe B. Owen H. Malisano J. Martin D. Hofstetter J. et al. The in vivo and in vitro corrosion of high-purity magnesium and magnesium alloys WZ21 and AZ91. Corrosion Science 2013;75:354-66.
[4] Yang JX. Cui FZ. Lee IS. Zhang Y. Yin QS. Xia H. et al. In vivo biocompatibility and degradation behavior of Mg alloy coated by calcium phosphate in a rabbit model. Journal of biomaterials applications 2012;27:153-64.
[5] Witte F. Kaese V. Haferkamp H. Switzer E. Meyer-Lindenberg A. Wirth CJ. et al. In vivo corrosion of four magnesium alloys and the associated bone response. Biomaterials 2005;26:3557-63.
[6] Chai H. Guo L. Wang X. Gao X. Liu K. Fu Y. et al. In vitro and in vivo evaluations on osteogenesis and biodegradability of a beta-tricalcium phosphate coated magnesium alloy. Journal of biomedical materials research Part A 2011.
[7] Gu XN. Zheng YF. Chen LJ. Influence of artificial biological fluid composition on the biocorrosion of potential orthopedic Mg-Ca. AZ31. AZ91 alloys. Biomedical materials 2009;4:065011.
[8] Wong HM. Yeung KW. Lam KO. Tam V. Chu PK. Luk KD. et al. A biodegradable polymer-based coating to control the performance of magnesium alloy orthopaedic implants. Biomaterials 2010;31:2084-96.
[9] Witte F. Fischer J. Nellesen J. Crostack HA. Kaese V. Pisch A. et al. In vitro and in vivo corrosion measurements of magnesium alloys. Biomaterials 2006;27:1013-8.
[10] Mueller WD. Nascimento ML. Lorenzo de Mele MF. Critical discussion of the results from different corrosion studies of Mg and Mg alloys for biomaterial applications. Acta biomaterialia 2010;6:1749-55.
[11] Xu L. Yu G. Zhang E. Pan F. Yang K. In vivo corrosion behavior of Mg-Mn-Zn alloy for bone implant application. Journal of biomedical materials research Part A 2007;83:703-11.
[12] Zhang S. Zhang X. Zhao C. Li J. Song Y. Xie C. et al. Research on an Mg–Zn alloy as a degradable biomaterial. Acta biomaterialia 2010;6:626-40.
[13] Kraus T. Fischerauer SF. Hanzi AC. Uggowitzer PJ. Loffler JF. Weinberg AM. Magnesium alloys for temporary implants in osteosynthesis: in vivo studies of their degradation and interaction with bone. Acta biomaterialia 2012;8:1230-8.
[14] Fischerauer SF. Kraus T. Wu X. Tangl S. Sorantin E. Hanzi AC. et al. In vivo degradation performance of micro-arc-oxidized magnesium implants: a micro-CT study in rats. Acta biomaterialia 2013;9:5411-20.
[15] Witte F. Fischer J. Nellesen J. Vogt C. Vogt J. Donath T. et al. In vivo corrosion and corrosion protection of magnesium alloy LAE442. Acta biomaterialia 2010;6:1792-9.
[16] Ullmann B. Reifenrath J. Dziuba D. Seitz J-M. Bormann D. Meyer-Lindenberg A. In Vivo Degradation Behavior of the Magnesium Alloy LANd442 in Rabbit Tibiae. Materials Letters 2011;4:2197-218.

[17] Hampp C. Ullmann B. Reifenrath J. Angrisani N. Dziuba D. Bormann D. et al. Research on the Biocompatibility of the New Magnesium Alloy LANd442-An In Vivo Study in the Rabbit Tibia over 26 Weeks. Advanced Engineering Materials 2012;14:B28-B37.
[18] Huehnerschulte TA. Angrisani N. Rittershaus D. Bormann D. Windhagen H. Meyer-Lindenberg A. In Vivo Corrosion of Two Novel Magnesium Alloys ZEK100 and AX30 and Their Mechanical Suitability as Biodegradable Implants. Materials Science and Engineering 2011;4:1144-67.
[19] Dziuba D. Meyer-Lindenberg A. Seitz JM. Waizy H. Angrisani N. Reifenrath J. Long-term in vivo degradation behaviour and biocompatibility of the magnesium alloy ZEK100 for use as a biodegradable bone implant. Acta biomaterialia 2013;9:8548-60.
[20] Wang Y. Zhu Z. He Y. Jiang Y. Zhang J. Niu J. et al. In vivo degradation behavior and biocompatibility of Mg-Nd-Zn-Zr alloy at early stage. International journal of molecular medicine 2012;29:178-84.
[21] Aghion E. Levy G. Ovadia S. In vivo behavior of biodegradable Mg-Nd-Y-Zr-Ca alloy. Journal of materials science Materials in medicine 2012;23:805-12.
[22] Li Z. Gu X. Lou S. Zheng Y. The development of binary Mg-Ca alloys for use as biodegradable materials within bone. Biomaterials 2008;29:1329-44.
[23] Yanjin LU LT. Hongliang XIANG. Bingchun ZHANG. Ke YANG. Study on corrosion resistance of pure magnesium with CaSiO3 contained coating in NaCl solution. Acta Metallurgica Sinica(English letters) 2012;25:287-94.
[24] Wang H. Shi Z. In vitro biodegradation behavior of magnesium and magnesium alloy. Journal of biomedical materials research Part B. Applied biomaterials 2011;98:203-9.
[25] Wang Y. He Y. Zhu Z. Jiang Y. Zhang J. Niu J. et al. In vitro degradation and biocompatibility of Mg-Nd-Zn-Zr alloy. Chinese Science Bulletin 2012;57:2163-70.
[26] Song G, Atrens A, Dargusch M. Influence of microstructure on the corrosion of diecast AZ91D. Corrosion Science 1999;41:249-73.
[27] Shi Z, Liu M, Atrens A. Measurement of the corrosion rate of magnesium alloys using Tafel extrapolation. Corrosion Science 2010;52:579-88.
[28] Gu X, Zheng Y, Cheng Y, Zhong S, Xi T. In vitro corrosion and biocompatibility of binary magnesium alloys. Biomaterials 2009;30:484-98.
[29] Wen Z, Wu C, Dai C, Yang F. Corrosion behaviors of Mg and its alloys with different Al contents in a modified simulated body fluid. Journal of Alloys and Compounds 2009;488:392-9.
[30] Ren Y. Huang J. Zhang B. Yang K. Preliminary study of biodegradation of AZ31B magnesium alloy. Frontiers of Materials Science in China 2007;1:401-4.
[31] Pardo A, Feliu S, Merino MC, Arrabal R, Matykina E. Electrochemical Estimation of the Corrosion Rate of Magnesium/Aluminium Alloys. International Journal of Corrosion 2010;2010.
[32] Gray-Munro JE. Seguin C. Strong M. Influence of surface modification on the in vitro corrosion rate of magnesium alloy AZ31. Journal of biomedical materials research Part A 2009;91:221-30.
[33] Salahshoor M. Guo Y. Biodegradable Orthopedic Magnesium-Calcium (MgCa) Alloys. Processing. and Corrosion Performance. Materials 2012;5:135-55.
[34] Mueller WD. de Mele MF. Nascimento ML. Zeddies M. Degradation of magnesium and its alloys: dependence on the composition of the synthetic biological media. Journal of biomedical materials research Part A 2009;90:487-95.

[35] Wu G, Fan Y, Gao H, Zhai C, Zhu YP. The effect of Ca and rare earth elements on the microstructure, mechanical properties and corrosion behavior of AZ91D. Materials Science and Engineering: A 2005;408:255-63.
[36] Zhou W, Shen T, Aung NN. Effect of heat treatment on corrosion behaviour of magnesium alloy AZ91D in simulated body fluid. Corrosion Science 2010;52:1035-41.
[37] Huan ZG. Leeflang MA. Zhou J. Fratila-Apachitei LE. Duszczyk J. In vitro degradation behavior and cytocompatibility of Mg-Zn-Zr alloys. Journal of materials science Materials in medicine 2010;21:2623-35.
[38] Li N. Guo C. Wu YH. Zheng YF. Ruan LQ. Comparative study on corrosion behaviour of pure Mg and WE43 alloy in static. stirring and flowing Hank's solution. Corrosion Engineering Science and Technology 2012;47:346-51.
[39] Rosalbino F. De Negri S. Scavino G. Saccone A. Microstructure and in vitro degradation performance of Mg-Zn-Mn alloys for biomedical application. Journal of biomedical materials research Part A 2013;101:704-11.
[40] Schinhammer M. Hofstetter J. Wegmann C. Moszner F. Löffler JF. Uggowitzer PJ. On the Immersion Testing of Degradable Implant Materials in Simulated Body Fluid: Active pH Regulation Using CO2. Advanced Engineering Materials 2013;15:434-41.
[41] Seitz J-M. Collier K. Wulf E. Bormann D. Bach F-W. Comparison of the Corrosion Behavior of Coated and Uncoated Magnesium Alloys in an In Vitro Corrosion Environment. Advanced Engineering Materials 2011;13:B313-B23.
[42] Mao L. Yuan G. Niu J. Zong Y. Ding W. In vitro degradation behavior and biocompatibility of Mg–Nd–Zn–Zr alloy by hydrofluoric acid treatment. Materials Science and Engineering: C 2013;33:242-50.
[43] Aghion E. Levy G. The effect of Ca on the in vitro corrosion performance of biodegradable Mg–Nd–Y–Zr alloy. Journal of materials science Materials in medicine 2010;45:3096-101.
[44] Yun Y. Dong Z. Yang D. Schulz MJ. Shanov VN. Yarmolenko S. et al. Biodegradable Mg corrosion and osteoblast cell culture studies. Materials Science and Engineering: C 2009;29:1814-21.
[45] Wang Y. Liu G. Fan Z. A new heat treatment procedure for rheo-diecast AZ91D magnesium alloy. Scripta Materialia 2006;54:903-8.
[46] Bobby Kannan M. Singh RK. A mechanistic study of in vitro degradation of magnesium alloy using electrochemical techniques. Journal of biomedical materials research Part A 2010;93:1050-5.
[47] Feyerabend F. Fischer J. Holtz J. Witte F. Willumeit R. Drucker H. et al. Evaluation of short-term effects of rare earth and other elements used in magnesium alloys on primary cells and cell lines. Acta biomaterialia 2010;6:1834-42.
[48] Mueller WD. Lucia Nascimento M. Lorenzo de Mele MF. Critical discussion of the results from different corrosion studies of Mg and Mg alloys for biomaterial applications. Acta biomaterialia 2010;6:1749-55.
[49] Reifenrath J. Krause A. Bormann D. von Rechenberg B. Windhagen H. Meyer-Lindenberg A. Profound differences in the in-vivo-degradation and biocompatibility of two very similar rare-earth containing Mg-alloys in a rabbit model. . Materialwissenschaft und Werkstofftechnik 2010;41:1054-61.
[50] Xin Y. Huo K. Tao H. Tang G. Chu PK. Influence of aggressive ions on the degradation behavior of biomedical magnesium alloy in physiological environment. Acta biomaterialia 2008;4:2008-15.

[51] Oyane A. Kim HM. Furuya T. Kokubo T. Miyazaki T. Nakamura T. Preparation and assessment of revised simulated body fluids. Journal of biomedical materials research Part A 2003;65:188-95.